

RESEARCH ARTICLE

Open Access

Functional connectivity changes in cerebral small vessel disease - a systematic review of the resting-state MRI literature



Maximilian Schulz¹, Caroline Malherbe^{1,2}, Bastian Cheng¹, Götz Thomalla¹ and Eckhard Schlemm^{1*} 

Abstract

Background: Cerebral small vessel disease (CSVD) is a common neurological disease present in the ageing population that is associated with an increased risk of dementia and stroke. Damage to white matter tracts compromises the substrate for interneuronal connectivity. Analysing resting-state functional magnetic resonance imaging (fMRI) can reveal dysfunctional patterns of brain connectivity and contribute to explaining the pathophysiology of clinical phenotypes in CSVD.

Materials and methods: This systematic review provides an overview of methods and results of recent resting-state functional MRI studies in patients with CSVD. Following the Preferred Reporting Items for Systematic Reviews and Meta-Analysis (PRISMA) protocol, a systematic search of the literature was performed.

Results: Of 493 studies that were screened, 44 reports were identified that investigated resting-state fMRI connectivity in the context of cerebral small vessel disease. The risk of bias and heterogeneity of results were moderate to high. Patterns associated with CSVD included disturbed connectivity within and between intrinsic brain networks, in particular the default mode, dorsal attention, frontoparietal control, and salience networks; decoupling of neuronal activity along an anterior–posterior axis; and increases in functional connectivity in the early stage of the disease.

Conclusion: The recent literature provides further evidence for a functional disconnection model of cognitive impairment in CSVD. We suggest that the salience network might play a hitherto underappreciated role in this model. Low quality of evidence and the lack of preregistered multi-centre studies remain challenges to be overcome in the future.

Keywords: Brain network, Cerebral small vessel disease, Cognition, Functional connectivity, Magnetic resonance imaging, Resting state, Risk of bias, Patho-connectomics, Systematic review

* Correspondence: e.schlemm@uke.de

¹Department of Neurology, University Medical Centre Hamburg-Eppendorf, Hamburg, Germany

Full list of author information is available at the end of the article



© The Author(s). 2021 **Open Access** This article is licensed under a Creative Commons Attribution 4.0 International License, which permits use, sharing, adaptation, distribution and reproduction in any medium or format, as long as you give appropriate credit to the original author(s) and the source, provide a link to the Creative Commons licence, and indicate if changes were made. The images or other third party material in this article are included in the article's Creative Commons licence, unless indicated otherwise in a credit line to the material. If material is not included in the article's Creative Commons licence and your intended use is not permitted by statutory regulation or exceeds the permitted use, you will need to obtain permission directly from the copyright holder. To view a copy of this licence, visit <http://creativecommons.org/licenses/by/4.0/>. The Creative Commons Public Domain Dedication waiver (<http://creativecommons.org/publicdomain/zero/1.0/>) applies to the data made available in this article, unless otherwise stated in a credit line to the data.

Background

Cerebral small vessel disease (CSVD) is a term that describes clinical, neuroimaging, and pathological features assumed to arise from compromised blood flow in the intrinsic cerebral arteriolar system [1]. In its later stages, CSVD is associated with neurological symptoms, in particular lacunar ischaemic stroke, and cognitive impairment ranging from mild deficits to vascular dementia [2, 3]. Small vessel disease is estimated to be the main etiological factor in up to 23% of all ischaemic strokes [4] and to be the second most common contributing factor to dementia after Alzheimer's pathology [5] and is thus responsible for a growing disease burden in ageing societies.

Even in its pre-symptomatic stage, CSVD is associated with structural brain changes on neuroimaging, in particular white matter hyperintensities (WMH) of presumed vascular origin, lacunes, cerebral microbleeds, enlarged perivascular spaces, and brain atrophy [6]. Cardiovascular risk factors, such as hypertension, diabetes, smoking, or dyslipidaemia, are associated with both WMH and the clinical sequelae associated with CSVD [7, 8].

In recent years, the network perspective on the human brain has revolutionised neuroscience and advanced our understanding of neurological and psychiatric disorders [9–12]. The network paradigm posits that different brain regions, while spatially remote, are structurally and functionally linked and interact to facilitate brain functions. Analysis of structural brain networks by magnetic resonance diffusion tensor imaging revealed that WMH disrupts the topological organisation of the brain connectome and that the associated loss of network efficiency links vascular risk burden and cognitive impairment [13–16]. Nevertheless, there remains considerable variability in clinical phenotypes, such as cognitive impairment or affective functions, that is not explained by structural markers alone [17–19].

Functional connectivity (FC), on the other hand, is defined as the pattern of synchronous neuronal activation [20], which, in turn, can be probed *in vivo* using the blood-oxygen level-dependent (BOLD) signal in magnetic resonance imaging (MRI) [21]. Functional connectivity can be analysed either in response to tasks and external stimuli or in the resting-state which minimises the cognitive and behavioural demand on subjects [21]. The latter provides a description of the spatiotemporal organisation of brain activity, from which discrete modes can be extracted as intrinsic resting-state networks that correspond to specific cognitive domains [22].

Recently, the benefits of such a shift of perspective toward a more global understanding of brain function have also been recognised for cerebral small vessel disease [23]. While the clinical benefits of

understanding patterns of disrupted FC associated with CSVD might seem, at the moment, very limited, our vision is that, ultimately, it might contribute to designing and implementing patient-specific interventions in the form of neuropsychological training or electromagnetic stimulation to help ameliorate cognitive impairment. Evidence for the relevance of disturbed connectivity especially in the default mode, dorsal attention, and frontoparietal control networks to cognitive impairment in CSVD has been reviewed previously, covering the literature up to 2014 [24]. In the present article, we provide an overview over the rapidly expanding recent literature on altered resting-state connectivity patterns associated with CSVD. In contrast to previous work, we include studies of both clinically healthy individuals and patients with manifest CSVD and consider both distributed networks and point-to-point connectivity. In order to keep the review focused, we restrict attention to resting-state functional MRI studies and do not review studies using a task-based design or different imaging modalities, such as electro- or magnetoencephalography. The goal is to take stock of the current literature, review methodological advances in recent years, and update our understanding of the neural mechanisms underlying the cognitive deficits that patients with CSVD face.

Methods

A systematic review of the literature was performed according to the Preferred Reporting Items for Systematic Reviews and Meta-Analysis (PRISMA) statement [25]; the protocol for the review was not preregistered.

Literature search and study selection

Inclusion criteria for articles considered in this review were as follows: (1) written in English, (2) analysing exclusively human study participants, (3) published after January 2010, (4) radiological evidence of sporadic cerebral small vessel disease with structural brain imaging showing manifestations of CSVD in the form of white matter hyperintensities in at least a subset of the study population, and (5) analysis of resting-state functional connectivity using functional MRI. We excluded review articles; descriptions of ongoing studies; functional imaging studies using only electroencephalography, magnetoencephalography, or positron emission tomography; and reports concentrating exclusively on patients with non-sporadic CSVD, e.g. of genetic origin, or non-vascular dementias, e.g. Alzheimer's disease.

Following a prespecified search strategy, the PubMed online database was queried for studies published between January 2010 and November 2020 using the conjunction of keywords specific for pathology ('small

vessel disease', 'white matter lesion', 'leukoaraiosis', 'microangiopathy'), network science ('connectivity', 'network', 'graph', 'module'), and imaging modality ('MRI', 'BOLD', 'resting state') as search criteria (see Additional file 1 for the exact search strategy). In addition, references of search results were screened for further eligible articles. Studies were discarded if the title or abstract indicated failure to meet all the specified inclusion or satisfaction of at least one exclusion criterion. The remaining articles were read in full and evaluated according to the stated criteria.

The risk of methodological bias in individual studies (PRISMA items 12 and 19) was assessed using the Appraisal tool for Cross-Sectional Studies (AXIS tool) [26], modified to not contain items related to presentation of the Results, the Discussion of findings, or the Funding of the study [27]. Detailed descriptions of individual items are presented in Additional file 1: Table S1. Based on the number of quality criteria satisfied, each study was assigned an integer score from 0 (no criteria satisfied) to 11 (all criteria satisfied). Trichotomising this ordinal scale, we classified the risk of bias as high (score 0–3), moderate (4–7), or low (8–11). We strived to cover the literature comprehensively, and even a high risk of bias was therefore not defined as an exclusion criterion for this review.

Data extraction and analysis

After screening, the following data were extracted from the articles: year of publication; sample size; average age and clinical characteristics of study populations including measures undertaken to minimise confounding by comorbidities; the employed operationalisation of cerebral small vessel disease and severity grading of WMH; details of the scanning parameters and pre-processing steps including the controversial topics of motion scrubbing and global signal regression; the analytical approach to functional connectivity; and key results regarding patterns of altered connectivity in patients with CSVD and, if reported, their relation to cognitive performance.

For ease of presentation, studies were classified according to clinical characteristics of the study population—manifest CSVD, healthy participants, or others, not primarily vascular clinical conditions—and their main approach to quantifying and analysing connectivity. These predefined analytical categories included short-range connectivity within a part of the brain, long-range connectivity between pairs of remote brain areas defined either a priori or using a data-driven approach, and global analyses of topological properties of the functional connectome. We also reviewed the cognitive tests applied in these studies and

associations of cognitive ability with functional connectivity measurements.

Results

Study characteristics

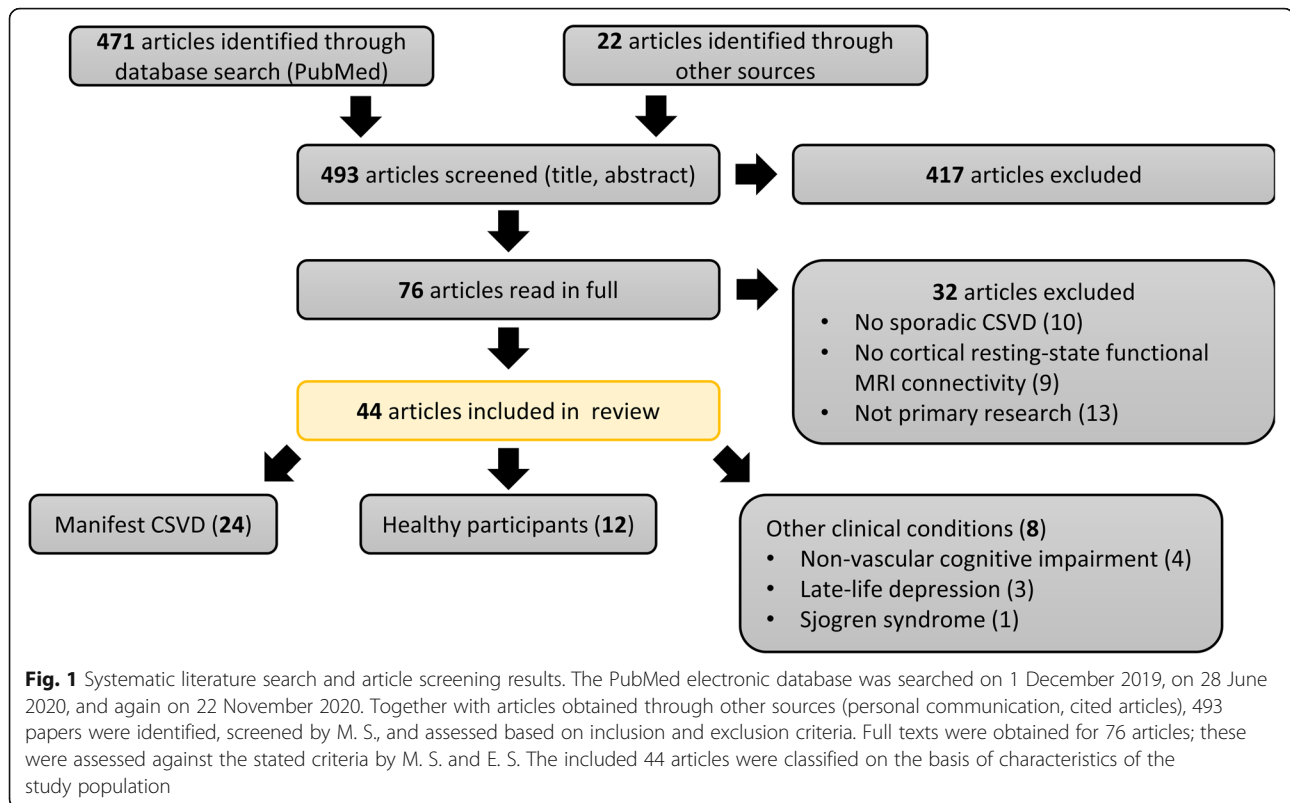
The results of the search and selection process are summarised in Fig. 1. We identified a total of 493 potentially relevant papers, 471 of which were obtained by searching PubMed and 22 through personal communication or as references cited in other works. Four hundred seventeen papers were excluded based on their title or abstract. Of the remaining 76 studies, which were read in full by both MS and ES, 44 were included in this review. Details of individual studies are summarised in Table 1.

The number of subjects, including both patients with small vessel disease and controls depending on study design, varied between 11 and 1584 with a median sample size of 72.5 (interquartile range [IQR] 50.8–106.8). Mean age across studies ranged from 50.0 to 76.4 years, with a median of 66.0 years (IQR 62.4–69.8 years).

Regarding the underlying research questions, roughly half of the included studies (24/44) reported the investigation of altered functional connectivity patterns in the presence of cerebral small vessel disease and its relation to cognitive ability as their primary research objective. Of these, six reports focused on patients with CSVD exclusively, whereas the study designs of the remaining reports involved comparing groups of healthy controls, patients with non-vascular cognitive impairment, or both. Twelve studies reported measures of cerebral small vessel disease, often as part of a more comprehensive assessment of structural brain parameters, and functional connectivity in populations of healthy participants without clinically manifest vascular pathology or cognitive impairment. Eight articles addressed functional connectivity in the context of other clinical conditions not directly related to vascular pathology, such as tau pathology-associated cognitive impairment or depression, but included markers of small vessel disease as covariates.

Operationalisation of CSVD and associated cognitive impairment

All of the 24 MRI studies reporting on resting-state functional connectivity in the context of clinically overt CSVD defined the presence of white matter hyperintensities on T2-weighted cerebral MR imaging as one of their inclusion criteria. In more than half of the studies (14/24), these were evaluated according to the ordinal Fazekas scale [55, 56]; in three studies, authors chose the Wahlund scale to assess age-related white matter changes [32]; white matter lesion load was also quantified volumetrically in eight studies; no precise definition of imaging criteria was reported in five articles.



When white matter disease was reported as a structural covariate in the investigation of functional connectivity, the extent of structural changes was quantified using either absolute or relative white matter hyperintensity volumes. Techniques for segmenting WMH on either T2 or FLAIR sequences included manual, semi-manual, and fully automated approaches; in one case, the algorithm was not described [57].

Beyond the presence of white matter lesions, evidence of lacunes or recent lacunar infarcts was considered in 13/24 studies; the distinction between the two entities was often imprecise, with only three articles referring to the Standards for Reporting Vascular changes on neuroimaging (STRIVE, [6]) consensus statement in this context [31, 50, 51]. Reflecting their conceptualisation as fluid-filled cavities, lacunes were defined as hypointense ovoid regions on T2- or FLAIR-weighted imaging with a diameter ranging from [2–3] to [15–20] mm. Three studies required patients with CSVD to have evidence of at least one lacuna or recent lacunar infarct [28, 42, 52], while one report excluded such patients [36]. Information on the number of lacunes contributed to the definition of a composite CSVD score in one study [49]; in the remaining cases, it was either reported descriptively or used as a covariate in statistical analyses [50]. While most studies specified cortical or large subcortical

infarcts as an exclusion criterion, one article included such patients specifically [43].

In addition to imaging findings, clinical characteristics were used to define patient cohorts. This was done to either separate patients and participants with and without cognitive impairment; to differentiate patients with CSVD from patients with non-vascular cognitive impairment, especially Alzheimer's disease; or to grade the severity of vascular cognitive impairment, ranging from cognitively normal (CN) over mildly affected (variably called *subcortical vascular mild cognitive impairment* [svMCI], or *vascular cognitive impairment no dementia* [VICND]) to subcortical vascular dementia (SVaD). In addition to dedicated diagnostic criteria for different dementias [58, 59], cognitive assessment was based predominantly on scales such as the Mini Mental State Examination (MMSE), Montreal Cognitive Assessment battery (MoCA), or Clinical Dementia Rating scale (CDR). A minority of studies used the Petersen criteria and included functional activities and temporal evolution of cognitive abilities in their definition of mild cognitive impairment [60, 61]. Only three studies employed positron emission tomography (PET) to distinguish tau and/or amyloid pathology from purely vascular disease [49, 62, 63], and the risk of confounding by mixed disease seems therefore high in the majority of reported studies.

Table 1 Summary of included articles analysing resting-state functional connectivity in patients with manifest cerebral small vessel disease (CSVD). We report imaging and clinical characteristics of patients included in each study, key steps in the acquisition and pre-processing of BOLD data, analysis of functional connectivity, and FC patterns found to be associated with CSVD. Descriptive statistics as extracted from articles are reported as mean \pm standard deviation. Missing information is indicated by empty brackets (). Arrows indicate increased (↑) or reduced (↓) values, as well as positive (↗) and negative (↘) associations

Reference	Participants with CSVD	Characteristics of patients with CSVD		MRI acquisition params	BOLD pre-processing	FC analysis	FC patterns associated with CSVD	Risk of bias (AXIS)
		Neuroimaging	Cognition					
[28]	18 CSVD-CN 16 CSVD-MCI	WMH and lacunes (clinical diagnosis)	MMSE CN 28.9 \pm 1.3 MCI 28.1 \pm 1.4	Philips Achieva, 3 T TR 2000 ms, TE 30 ms 64 \times 64 \times [] 3.6 \times 3.6 \times 4 mm ³ 220 volumes eyes open	DPARSF v2.0, SPM 5, REST [Confound regression] Motion scrubbing - Max motion > 1 mm/1°	PCC from external template SCA to define DMN Pearson correlation	↓ FC in DMN in the left middle temporal gyrus, left ant. cingulate/left middle frontal gyrus, right caudate, right middle frontal gyrus, and left medial frontal gyrus/paracentral lobule ↑ FC in DMN in the right inf. temporal gyrus, left middle temporal gyrus, left precentral gyrus, and left sup. parietal lobule	High (2)
[29]	29 CSVD	WMH (clinical diagnosis) WMH volume VRF 0, 20.4 \pm 19.3 VRF 1, 27.3 \pm 21.5 VRF 3, 17.4 \pm 19.5	MoCA VRF 0, 25.8 \pm 3.5 VRF 1, 22.0 \pm 6.2 VRF 3, 21.0 \pm 5.4	Philips Achieva, 3 T TR 2000 ms, TE 30 ms 64 \times 64 \times 40 3.6 \times 2.9 \times 3 mm ³ 184–259 volumes, [eyes]	FSL v4.1 Confound regression - ICA Motion scrubbing - 'relative motion' > 1.5 mm	ICA to define DMN, SMN, medial-visual RSN Pearson correlation	FC in DMN ↗ cardiovascular reactivity	Moderate (4)
[30]	21 CSVD-CN 16 CSVD-MCI 13 SVaD	WMH (clinical diagnosis)	MMSE CN 28.9 \pm 0.7 MCI 26.3 \pm 1.0 SVaD 20.5 \pm 2.3 MoCA CN 24.6 \pm 2.9 MCI 20.6 \pm 2.8 SVaD 15.1 \pm 3.6	Siemens, 3 T TR 2480 ms, TE 30 ms 64 \times 64 \times 36, 3 \times 3 \times 4 mm ³ 240 volumes eyes closed	SPM 8 [Confound regression] Motion scrubbing - Head motion > 2 mm/2°	AAL atlas Pearson correlation, (extended) maximal information coefficient SVM classification	None	High (3)
[31]	46 CSVD 41 CADASIL	WMH volume 0.3% [0-03, 3.11% of intracranial volume Lacunes 0 (0) [0–20]	MMSE median 29, IQR [26, 32]	Siemens Skyra/Prisma, 3 T, 64-/32-channel head coils, multi-band \times 8 TR 700 ms, TE 39 ms [matrix] 3 \times 3 \times 3 mm ³ 2.4 \times 2.4 \times 2.4 mm ³ 675–700 volumes eyes closed	FSL, ANTs, BRAMILA v2.0 Confound regression - ICA-AROMA non-aggressive - Linear trend, 6 motion params - GSR: CSF, WM Motion scrubbing - Volume censoring (FD > 0.5 mm, total time < 5 min)	Power atlas to define DMN, FPCN, hand-SMN, VN Pearson correlation graph theory	No association between WMH and FC Poor reproducibility of network measures in CSVD	Moderate (6)

Table 1 Summary of included articles analysing resting-state functional connectivity in patients with manifest cerebral small vessel disease (CSVD). We report imaging and clinical characteristics of patients included in each study, key steps in the acquisition and pre-processing of BOLD data, analysis of functional connectivity, and FC patterns found to be associated with CSVD. Descriptive statistics as extracted from articles are reported as mean ± standard deviation. Missing information is indicated by empty brackets (). Arrows indicate increased (↑) or reduced (↓) values, as well as positive (↗) and negative (↘) associations (*Continued*)

Reference	Participants	Characteristics of patients with CSVD		MRI acquisition params	BOLD pre-processing	FC analysis	FC patterns associated with CSVD	Risk of bias (AXIS)
		Neuroimaging	Cognition					
[33]	33 MCI with confluent (C) WMH 30 MCI with non-confluent (NC) WMH	Fazekas C-WMH 8.0 ± 2.4 NC-WMH 3.2 ± 1.2 WMH volume C-WMH 8.7 ± 9.2 ml NC-WMH 1.9 ± 1.5 ml	MMSE C-WMH 27.6 ± 1.5 NC-WMH 27.8 ± 1.7	Siemens Trio, 3 T TR 2000 ms, TE 30 ms □ × [□ × 36, 3 × 3 × 3 mm ³ 240 volumes [eyes]	CONN 18b Confound regression - GSR: WM, CSF - Motion parameters Motion correction - Artefact Detection Tools - Spike regression (FD > 0.5 mm)	CONN atlas with 138 ROIs to define DMN, SMN, VN, DAN, FPCN language, and cerebellar networks Bivariate correlation coefficients	↑ Interregional FC (C-WMH > NC-WMH) ↑ Intra-regional FC (C-WMH > NC-WMH) Few ↓ interregional FC (C-WMH < NC-WMH)	High (2)
[34]	29 CSVD with gait disorder (GD+) 29 CSVD without gait disorder (GD-)	Fazekas ≥ 2 WMH volume GD+, 6.12 mm ³ GD-, 3.53 mm ³ Lacunes GD+, 7.45 ± 4.01 GD-, 5.62 ± 3.35	MMSE GD+, 25.14 ± 3.24 GD-, 25.69 ± 3.32	GE Signa, 3 T, 8-channel head coil TR 2000 ms, TE 30 ms 64 × 64 × [] 3.75 × 3.75 × 4.6 mm ³ 240 volumes eyes closed	DPABI, SPM 8 Confound regression - Linear trend, 24p - GSR: CSF, WM Motion scrubbing - 'displacement' > 2.5 mm /2.5°	fALFF Pearson correlation VBM	↓ FC between left SMA and temporal lobe (GC+ < GD-) ↗ gait speed fALFF in left SMA ↗ cadence	Moderate (4)
[35]	12 CSVD 21 HC	Wahlund 8.3 ± 4.0 Lacunes 1.9 ± 2.4	1.5	Healthy controls and patients with CSVD without mandatory cognitive impairment [Scanner, field str.] TR 2300 ms, [TE] [matrix], 3 × 3 × 4 mm ³ 300 volumes [eyes]	FSL, AFNI, SPM B ₀ field map correction Confound regression - Linear/quadratic trend - 6 motion parameters - GSR, WM, CSF signal [Motion scrubbing]	Eigenvector centrality	↓ FC in ventromedial PFC, MCC, and sup. parietal lobe ↑ FC in the cerebellar regions I-VI FC ↗ WMH in the middle temporal sulcus, inf. temporal gyrus, cerebellar lobules Crus II, VIIb, VIII FC ↘ WMH in ventromedial PFC, SMA, PCC, and sup. parietal lobe	High (1)
[36]	30 CSVD 26 HC	Fazekas 1-3 Lacunes excluded	MoCA 22.9 ± 3.4 (pooled)	Siemens, 3 T TR 2480 ms, TE 30 ms 64 × 64 × 36, 3 × 3 × 4 mm ³ 240 volumes, eyes closed	SPM 8 [Confound regression] Motion scrubbing - Head movement > 2 mm/2°	ICA to define SMN voxel-wise two-sample t test	↓ FC in the right cingulate motor area, left posterior insula, and left ventral premotor area	High (2)
[37]	28 CSVD 30 HC	Fazekas 2.9 ± 1.2	MMSE 27.9 ± 1.6 MoCA 25.7 ± 2.0	Siemens Trio, 3 T TR 2000 ms, TE 30 ms 64 × 64 × [] 3.5 × 3.5 × 3 mm ³ 240 volumes [eyes]	SPM 8, DPABI, REST [Confound regression] Motion scrubbing - Head movement > 2 mm/2°	ALFF, SCA	↓ ALFF in the left parahippocampus and right frontal sup. orbital gyrus ↑ FC between right insula-right sup. orbitofrontal gyrus and right calcarine-left parahippoc. gyrus	High (2)

Table 1 Summary of included articles analysing resting-state functional connectivity in patients with manifest cerebral small vessel disease (CSVD). We report imaging and clinical characteristics of patients included in each study, key steps in the acquisition and pre-processing of BOLD data, analysis of functional connectivity, and FC patterns found to be associated with CSVD. Descriptive statistics as extracted from articles are reported as mean \pm standard deviation. Missing information is indicated by empty brackets (). Arrows indicate increased (↑) or reduced (↓) values, as well as positive (↗) and negative (↘) associations (Continued)

Reference	Participants	Characteristics of patients with CSVD	MRI acquisition params	BOLD pre-processing	FC analysis	FC patterns associated with CSVD	Risk of bias (AXIS)
		Neuroimaging					
		Cognition					
[38]	16 CSVD 13 HC	WMH (clinical diagnosis, Fazekas) MMSE 23.7 \pm 3.9 MoCA 18.3 \pm 4.1	Siemens, 3 T TR 2000 ms, TE 30 ms 64 \times 64 \times 35 3 \times 3 \times 3 mm ³ 230 volumes eyes closed	SPM 8 Confound regression - Linear trend Motion scrubbing - Head movement > 2 mm/2°	Regional homogeneity	↓ ReHo in the left insula, right sup. temporal gyrus, Rolandic operculum, precentral gyrus, and cerebellum; bilateral ant. cingulate gyrus, ant. MCC, PFC, and SMA ↑ ReHo values in the left middle temporal gyrus, cuneus and sup. occipital gyrus, and the bilateral angular gyrus, precuneus, postcentral gyrus, inf. and sup. parietal gyrus	Moderate (5)
[39]	15 CSVD 15 HC	WMH (clinical diagnosis, Fazekas) MMSE 23.7 \pm 4.0 MoCA 18.6 \pm 4.1	Siemens, 3 T TR 2000 ms, TE 30 ms 64 \times 64 \times [] 3 \times 3 \times 4 mm ³ 230 volumes eyes closed	DPABI v2.1 Confound regression - Linear trend - 24p [40] - GSR: WM, CSF - Spike regressor (FD > 0.2 mm) Motion scrubbing - Mean FD > group mean + 2*SD	36 ROIs representing DMN, DAN, FPCN, SMN, VN Pearson correlation Network-based statistics (NBS) [41]	↓ AN-SMN network FC ↑ DAN-FPCN network FC ↓ Edge FC SMN-AN, SMN-VN, FPCN-AN and DAN-VN pairs, and within AN and VN ↑ Edge FC in DMN-AN, DMN-FPCN, and DAN-FPCN pairs	High (3)
[42]	26 lacunar stroke patients 19 HC	Fazekas \geq 2 Lacunes 1–17 WMH 33 \pm 34 ml History of lacunar stroke syndrome	Siemens Verio, 3 T, 32-channel head coil TR 2430 ms TE 17/2/3 13/31/48 ms 64 \times 64 \times 34 3.75 \times 3.75 \times 4.18 mm ³ 269 volumes, eyes open	SPM, CONN Confound regression - Motion parameters [details] - GSR: WM, CSF [Motion scrubbing]	Desikan–Killiany parcellation Pearson correlation Probab. tractography Graph theory	No difference in FC or brain network topology	Moderate (6)
[43]	36 CSVD 31 HC	Fazekas \geq 2 MMSE HC 28.4 \pm 1.8 CSVD 26.4 \pm 3.7	Siemens Verio, 3 T, 12-channel head coil TR 2000 ms, TE 25 ms 64 \times 64 \times [z] 3.75 \times 3.75 \times 4 mm ³ [volumes], [eyes]	DPARSF, SPM 8 Confound regression - 6 head motions - GSR: global, WM, CSF Motion scrubbing - Head movement > 2 mm/2°	AAL 90 Pearson correlation Graph theory NBS	↓ Global FC ↑ Characteristic path length ↓ Global efficiency	High (0)

Table 1 Summary of included articles analysing resting-state functional connectivity in patients with manifest cerebral small vessel disease (CSVD). We report imaging and clinical characteristics of patients included in each study, key steps in the acquisition and pre-processing of BOLD data, analysis of functional connectivity, and FC patterns found to be associated with CSVD. Descriptive statistics as extracted from articles are reported as mean \pm standard deviation. Missing information is indicated by empty brackets (). Arrows indicate increased (↑) or reduced (↓) values, as well as positive (↗) and negative (↘) associations (Continued)

Reference	Participants	Characteristics of patients with CSVD		MRI acquisition params	BOLD pre-processing	FC analysis	FC patterns associated with CSVD	Risk of bias (AXIS)
		Neuroimaging	Cognition					
Healthy controls and patients with CSVD with mandatory cognitive impairment								
[44]	26 svMCI 28 HC	Wahlund ≥ 2 \pm lacunes	Subjective complaints MMSE 25.7 \pm 2.7	Siemens, 3 T TR 2000 ms, TE 40 ms 64 \times 64 \times 28 4 \times 4 \times 5 mm ³ 239 volumes eyes closed	SPM 5 Confound regression - Linear trend - 6 motion profiles - GSR: WM, CSF Motion scrubbing - Head movement > 3 mm/3°	ALFF, SCA, FC density Pearson correlation (only positive)	↓ ALFF in bilateral medial PFC ↑ ALFF in right PCC, precuneus, right hippocampus, right thalamus ↓ FC in DMN (PCC/precuneus, medial PFC, sup. frontal gyrus, inf. parietal lobule and hippocampus) and inferior/middle frontal gyrus	High (2)
[45]	21 svMCI 26 HC	Wahlund ≥ 2 \pm lacunes	Subjective complaints MMSE 25.5 \pm 2.7	Siemens, 3 T TR 2000 ms, TE 40 ms 64 \times 64 \times 28 4 \times 4 \times 5 mm ³ 239 volumes eyes closed	SPM 5 and 8, REST, DARTEL Confound regression - Linear trend - 6 motion profiles - GSR: WM, CSF Motion scrubbing - Head movement > 3 mm/3° - Volume censoring (FD > 0.3 mm, < 3 min)	H-1024 parcellation Pearson correlation Graph theory	↑ Characteristic path length, ↑ modularity ↑ Within-module degree in the medial PFC, left insula, and cuneus ↓ Within-module degree in the middle cingulate gyrus ↑ Participation coefficient in the left inferior/superior parietal cortex	High (1)
[46]	37 PIB+ AD 37 PIB- SVaD 13 mixed dementia 65 HC	Fazekas (severe)	MMSE PIB+ AD, 18.1 \pm 4.2 PIB- SVaD, 21.5 \pm 4.3 MD, 17.9 \pm 4.9 HC, 28.9 \pm 1.2	Philips Achieva, 3 T, 8-channel head coil TR 3000 ms, TE 35 ms [matrix], 1.7 \times 1.7 \times 4 mm ³ 100 volumes, eyes open	AFNI Despiking [Confound regression] Motion scrubbing - Max FD > 0.3 mm - Head movement > 2 mm/2°	ICA to define DMN and FPCN W-score maps	↓ FC in DMN in the left superior frontal gyrus ↓ FC in FPCN in the left insula	Moderate (5)
[47]	32 CSVD-CI 23 HC	Fazekas 2-3 \pm lacunes	MMSE 23.8 \pm 2.7	GE Signa, 3 T TR 2000 ms, TE 30 ms 64 \times 64 \times 4 3.75 \times 3.75 \times 4.6 mm ³ 240 volumes eyes closed	SPM 8, DPARSF, CONN Confound regression - compCor - GSR: global signal [Motion scrubbing]	Medial PFC and thalamus from ext. template SCA Pearson correlation	↓ FC between the left thalamus and right sup. temporal gyrus, left sup. frontal gyrus, left and putamen ↓ FC between the right thalamus and left inferior temporal gyrus ↑ FC between the bilateral thalamus and right inferior/middle frontal gyri ↓ FC between the med. PFC and bilateral SMA, thalamus, left sup. frontal gyrus, ACC, sup. parietal lobe, and hippocampus	High (2)

Table 1 Summary of included articles analysing resting-state functional connectivity in patients with manifest cerebral small vessel disease (CSVD). We report imaging and clinical characteristics of patients included in each study, key steps in the acquisition and pre-processing of BOLD data, analysis of functional connectivity, and FC patterns found to be associated with CSVD. Descriptive statistics as extracted from articles are reported as mean \pm standard deviation. Missing information is indicated by empty brackets (). Arrows indicate increased (↑) or reduced (↓) values, as well as positive (↗) and negative (↘) associations (Continued)

Reference	Participants	Characteristics of patients with CSVD	MRI acquisition params	BOLD pre-processing	FC analysis	FC patterns associated with CSVD	Risk of bias (AXIS)
		Neuroimaging					
		Cognition					
[48]	14 CSVD-CN 27 CSVD-MCI 12 SvAD 30 HC	MMSE Fazekas (cut-off not specified) CSVD-CN 29.1 \pm 1.0 CSVD-MCI 27.2 \pm 2.4 SvAD 23.3 \pm 3.4	Siemens, 3 T TR 2000 ms, TE 30 ms 64 \times 64 \times 32, 4 \times 4 \times 3.7 mm ³ [volumes], eyes closed	SPM 8 [Confound regression] Motion scrubbing - Head movement > 2 mm/2°	ICA to define DMN, SN, FPCN SCA from the right fronto-insular cortex	↓ FC between SN-DMN ↑ FC between SN-FPCN and within SN	High (3)
[49]	36 CSVD 50 AD 55 HC	MMSE svMCI 25.4 \pm 3.7 SvAD 17.4 \pm 4.2 10.1 ml Lacunes svMCI 6.5 \pm 7.5 SvAD 7.4 \pm 7.2 Microbleeds svMCI 13.4 \pm 18.7 SvAD 26.0 \pm 49.2	Siemens, 3 T TR 3000 ms, TE 35 ms [matrix] 3.4 \times 3.4 \times 3.4 mm ³ 200 volumes [eyes]	SPM 12 No smoothing Confound regression - Motion parameters - Linear trend - GSR: WM, CSF Motion scrubbing - Volume censoring (FD > 1 mm, > 30%)	Schaefer 400 atlas Pearson correlation AVI451 tau-PET	FC ↗ tau covariance, no associations with WMH	Moderate (7)
[50]	25 CSVD-CN 24 CSVD-MCI 36 HC	MMSE CN 28.4 \pm 1.3 MCI 27.8 \pm 2.1 MoCA CN 3.0 (0.76, 4.0) ml MCI 4.8 (0.76, 5.6) ml	Philips, 3 T TR 2000 ms, TE 30 ms 64 \times 64 \times 35 3.75 \times 3.75 \times 4 mm ³ 230 volumes eyes closed	GREYNA v2.0, SPM 8 Confound regression - Linear trend, 24p - GSR: GS, WM, CSF Motion scrubbing - Head movement > 2 mm/2°	H-1024 parcellation Pearson correlation Graph theory to define DMN, FPCN, SMN, and VN	No robust associations	Moderate (4)
[51]	21 CSVD-CN 20 CSVD-MCI 25 HC	MMSE CN 28.5 \pm 1.3 MCI 28.1 \pm 1.3 MoCA CN 25.6 \pm 1.9 MCI 22.2 \pm 2.9	Philips, 3 T, 32-channel head coil TR 2000 ms, TE 30 ms 64 \times 64 \times 35 3.75 \times 3.75 \times 4 mm ³ 230 volumes Eyes closed	DPABI Confound regression - 24p - GSR: GS, WM, CSF Motion scrubbing - Head movement > 3 mm/3°	PCC, dlPFC, IPS from external template SCA to define DMN, FPCN, and DAN	↓ FC in DMN in the right thalamus, hippocampus, and precuneus ↑ FC in FPCN in the right inf. parietal lobe ↓ FC between PCC-FPCN in the left precentral gyrus and bilateral middle cingulate gyri ↓ FC between PCC-DAN in the bilateral paracentral lobule and precuneus ↓ FC between PCC-DAN in the bilateral PCC and right precuneus	Moderate (6)

Table 1 Summary of included articles analysing resting-state functional connectivity in patients with manifest cerebral small vessel disease (CSVD). We report imaging and clinical characteristics of patients included in each study, key steps in the acquisition and pre-processing of BOLD data, analysis of functional connectivity, and FC patterns found to be associated with CSVD. Descriptive statistics as extracted from articles are reported as mean \pm standard deviation. Missing information is indicated by empty brackets (). Arrows indicate increased (\uparrow) or reduced (\downarrow) values, as well as positive (\rightarrow) and negative (\leftarrow) associations (*Continued*)

Reference	Participants with CSVD	Characteristics of patients with CSVD		MRI acquisition params	BOLD pre-processing	FC analysis	FC patterns associated with CSVD	Risk of bias (AXIS)
		Neuroimaging	Cognition					
[52]	14 CSVD + THA LAC	Fazekas 3–6 <i>Lacunes</i>	MMSE LAC+, 26.3 \pm 2.8	GE Discovery, 3 T TR 2000 ms, TE 35 ms 64 \times 64 \times 36	SPM 8 Confound regression - 6 motion parameters - GSR: WM, CSF	AAL 90 Pearson correlation Graph theory, Network-based statistics	\downarrow FC in para-/limbic and subcortical regions	Moderate (5)
	27 CSVD – THA LAC	LAC+, 5.6 \pm 3.9 LAC–, 2.0 \pm 1.4	LAC–, 28.1 \pm 2.0	3.4 \times 3.4 \times 4 mm ³ 210 volumes eyes closed	Motion scrubbing - Head movement > 2 mm/2°			
	34 HC							
[53]	32 CSVD+MCI 20 SvAd 35 HC	Fazekas \geq 1	MMSE MCI 25.5 \pm 1.8 SvAd 22.0 \pm 2.0 MoCA MCI 22.2 \pm 1. SvAd 17.4 \pm 2.9	Siemens Verio, 3 T TR 2000 ms, TE 30 ms 64 \times 64 \times 32 4 \times 4 \times 4.2 mm ³ 240 volumes eyes closed	DPARSF Confound regression - Linear/quadratic, 24p - GSR: WM, CSF Motion scrubbing - Head movement > 3 mm/3°	AAL atlas Pearson correlation Graph theory	\downarrow Global FC \downarrow Small-worldness	Moderate (4)
	20 LA-VAD 32 LA-VCIND 35 HC	Not reported	MMSE HC 29.4 \pm 1.1 LA-VCIND 27.9 \pm 1.8 LA-VaD 23.0 \pm 3.8 MoCA HC 26.0 \pm 2.5 LA-VCIND 25.8 \pm 2.0 LA-VaD 23.2 \pm 2.8	Siemens, 3 T TR 2000 ms, TE 30 ms 64 \times 64 \times 20 4 \times 4 \times 6 mm 250 volumes eyes closed	DPARSF Confound regression - 24p - GSR: WM, CSF Motion scrubbing - Head movement > 3 mm/3°	Group ICA (GIFT) Granger causality	Unclear; text and figures not consistent	High (2)

Functional MRI acquisition and pre-processing

Magnetic resonance imaging was performed on scanners from a variety of vendors (Siemens, Philips, GE), usually at 3 Tesla. The use of specialised receiver head coils, multi-band, or multi-echo techniques was rarely reported. Repetition time (TR) and echo time (TE) were predominantly set at 2000 ms and 30 ms, respectively, with exceptional values ranging from 700 to 4500 ms and 13 to 84 ms, respectively. Reconstructed voxel sizes in the BOLD scans varied in the range $[1.7\text{--}4] \times [1.7\text{--}4] \times [2\text{--}6] \text{ mm}^3$, arranged in a three-dimensional matrix of dimensions varying in the range $[64\text{--}128] \times [64\text{--}128] \times [20\text{--}64]$. The number of acquired BOLD volumes varied between 100 and 700 (median 230, IQR 180–240). Participants were asked to keep their eyes open in 12 and closed in 20 of the reviewed studies; 12 articles provided no information. Description of functional MRI acquisition parameters was incomplete in 26 of the 44 analysed studies (61%); methods were judged as not-repeatable in these cases (AXIS item 11). Hemodynamic lags were not considered.

Pre-processing steps common to most studies included slice-time correction; realignment to a reference volume to correct for head motion; normalisation to a template space (usually MNI EPI [64]) including resampling; temporal band-pass filtering (lower end 0.005–0.01 Hz; upper end 0.08–0.15 Hz); and smoothing with a Gaussian filter of full-width at half maximum (FWHM) between 4 and 8 mm.

Confound regression and motion scrubbing were performed and reported less uniformly, as detailed in Tables 1 and 2. Specifically, global signal regression (GSR), that is orthogonalisation of voxel-wise timeseries with respect to the average BOLD signals from the white and grey matter, or the whole brain, was undertaken in 27/44 studies. Twenty-five studies employed subject-wise censoring in which participants were excluded from further analysis if the maximum or average head translation or rotation during the scan exceeded a certain threshold ranging from 0.5 to 3 mm translation and 0.5 to 3° rotation. Ten studies performed volume censoring according to a framewise displacement (FD) or framewise translation/rotation cut-off, excluding participants with too few remaining uncontaminated volumes [31, 49]. Two studies used spike regression [39, 65].

Connectivity analysis

The majority of studies investigated large-scale functional connectivity between remote brain areas, choosing full or partial temporal correlations between the BOLD time courses as a measure of connectivity. Regions of interest were defined a priori using external brain parcellations in 16 cases. Twenty-seven studies used a data-driven approach such as independent component

analysis (ICA), seed-based connectivity analysis (SCA), or local BOLD activity (amplitudes of low-frequency fluctuations [ALFF]) to define regions of interest for further analysis. Many authors interpreted alterations in functional connectivity in the context of a small number of large-scale resting-state brain networks (RSNs), in particular the default mode (DMN) and frontoparietal control (FPCN) networks, but also the dorsal attention (DAN) and salience (SN) networks [22]. Eight reports used graph theoretical approaches, including global network parameters such as efficiency and clustering coefficient [31, 42, 43, 52, 53]; analysis of modularity structures [45, 50]; and self-referential quantification of region-specific centrality [35] to summarise the patterns of connectivity between multiple regions and to thus reflect global organisational principles of the brain networks.

Three studies investigated short-range connectivity [38, 66, 67], using regional homogeneity (ReHo) to quantify the similarity between BOLD signals as a marker of local connectivity [68].

The main findings of individual studies with respect to alterations in resting-state functional connectivity in the context of cerebral small vessel disease are summarised in Table 1. Patterns of altered connectivity were expressed either in comparison to healthy controls or along a gradient of increasing severity of CSVD imaging markers. For clinically or radiologically manifest CSVD, reduced functional connectivity dominated the findings on a global scale [43, 45, 53]. Within resting-state networks, lower functional coupling was repeatedly reported between components of the default mode network [28, 35, 44, 46, 47, 51], which is further supported by the co-occurrence of reduced DMN connectivity and increased WMH burden in patients with non-vascular cognitive impairment [62]. Within the FPCN, reduced connectivity was found in the left insula [46], whereas the right inferior parietal cortex appeared to be more strongly coupled to the rest of this network [51]. The average coupling between the DMN and FPCN was found to be reduced in patients with CSVD [51], even though a small number of inter-network edges showed increased connectivity [39]. The connectivity of the DAN was altered in relation to other networks with increased coupling to the FPCN and reduced coupling to the posterior DMN [39, 51]. The same pattern of altered inter-network connectivity was reported for the salience network [48]; intrinsic connectivity in the SN was increased in patients with CSVD and in association with the extent of white matter disease [83]. In healthy individuals or patients without symptomatic CSVD (Table 2), most studies did not report significant associations between FC and WMH burden [66, 79, 82, 86, 92]. Two studies found an association between higher FC,

Table 2 Summary of included articles analysing resting-state functional connectivity in healthy participants or patients without vascular cognitive impairment. We report imaging and clinical characteristics of patients included in each study, key steps in the acquisition and pre-processing of BOLD data, analysis of functional connectivity, and FC patterns found to be associated with CSVD. Descriptive statistics as extracted from articles are reported as range (min–max) and/or mean \pm standard deviation. Missing information is indicated by empty brackets ([]). Reported are clinical characteristics of patients included in each study, details about the quantification of white matter hyperintensities, key steps in the analysis of functional connectivity, and FC patterns found to be associated with CSVD. Arrows indicate increased (\uparrow) or reduced (\downarrow) values, as well as positive (\nearrow) and negative (\searrow) associations

Reference	Participants	Quantification of WMH load	rs-fMRI acquisition parameters	BOLD pre-processing	FC analysis	FC patterns associated with CSVD
[69]	12 depression 12 HC	Fuzzy connected algorithm [70]	GE Signa, 1.5T TR 2000 ms, TE 35 ms 64 × 64 × 26, 3.75 × 3.75 × 3.8 mm ³ [volumes], eyes open	AFNI [Confound regression] [Motion scrubbing]	PCC from ext. template SCA to define DMN Pearson correlation	FC in DMN \searrow WMH in medial PFC
[71]	47 depression 46 HC	Not reported	Siemens Trio, 3 T TR 2000 ms, TE 32 ms 128 × 128 × 28, 2 × 2 × 2 mm ³ 150 volumes, eyes open	SPM 5 [Confound regression] [Motion scrubbing]	PCC from ext. template SCA to define DMN Pearson correlation	\downarrow Association between DMN-FC and treatment response after controlling for WMH load
[62]	13 early AD 17 MCI 14 HC	Semi-automatic using FireVoxel [72]	[Scanner] TR 3000 ms, TE 30 ms [matrix], 3.3 × 3.3 × 3.3 mm ³ 140 volumes, [eyes]	[Confound regression] [Motion scrubbing]	Medial PFC and PCC from ext. atlas SCA to define DMN fALFF	Both increased WMH load and reduced DMN-FC in AD and MCI compared to HC
[73]	100 MCI	In-house automatic pipeline [74]	Philips Achieva, 3 T TR 2000 ms, TE 30 ms [matrix], [resolution] 200 volumes eyes closed	DPARSF Confound regression - 6 motion parameters - GSR: CSF, WM, global [Motion scrubbing]	SCA from the hippocampus and PCC	No association between WMH load and FC
[63]	43 MCI 24 HC	Histogram segmentation [75]	Training Philips, 3 T, 8-channel head coil TR 3000 ms, [TE] [matrix], 3.3 × 3.3 × 3.3 mm ³ 140 volumes eyes open Testing Siemens Verio, 3 T, 32-channel head coil TR 2580 ms, [TE] [matrix], 3.5 × 3.5 × 3.5 mm ³	DARTEL Confound regression - 6 motion parameters - GSR: CSF, WM [Motion scrubbing]	Whole-brain SCA Pearson correlation	No association between WMH and FC

Table 2 Summary of included articles analysing resting-state functional connectivity in healthy participants or patients without vascular cognitive impairment. We report imaging and clinical characteristics of patients included in each study, key steps in the acquisition and pre-processing of BOLD data, analysis of functional connectivity, and FC patterns found to be associated with CSVD. Descriptive statistics as extracted from articles are reported as range (min–max) and/or mean \pm standard deviation. Missing information is indicated by empty brackets (□). Reported are clinical characteristics of patients included in each study, details about the quantification of white matter hyperintensities, key steps in the analysis of functional connectivity, and FC patterns found to be associated with CSVD. Arrows indicate increased (↑) or reduced (↓) values, as well as positive (↗) and negative (↘) associations (*Continued*)

Reference	Participants	Quantification of WMH load	rs-fMRI acquisition parameters	BOLD pre-processing	FC analysis	FC patterns associated with CSVD
[65]	90 MCI 140 HC	SPM Lesion Segmentation Tool [76]	Siemens Trio, 3 T TR 2300 ms, TE 30 ms □ × □ × 34, 3 × 3 × 4 mm ³ [volumes] eyes closed	CONN, SPM 12 Confound regression - compCor - GSR: CSF, WM Motion scrubbing - Artefact Detection Tools - Spike regression (FD > 0.5 mm)	Preselected cognitive control networks (FPCN, SN) + DMN Pearson correlation Structural equation modelling	Weaker negative association between executive function/memory and WMH load in patients with high global FC
[77]	18 svMCI + depression 17 svMCI – depression 23 HC	Fazekas scale	GE MR750, 3 T TR 2000 ms, TE 35 ms 64 × 64 × 26, 4 × 4 × 4 mm ³ 240 volumes [eyes]	DPABI Confound regression - Linear and quadratic trends, 24p - GSR: CSF, WM, global Motion scrubbing - Head motion > 3 mm/3° - Volume censoring (FD > 0.5 mm)	SBM SCA from altered regions Pearson correlation	↑ FC between right middle cingulate cortex and right parahippocampal gyrus
[78]	38 P w Sjogren syndrome 40 HC	Wahlund score	Siemens Trio, 3 T TR 2500 ms, TE 30 ms 96 × 96 × 40, 2.3 × 2.3 × 3 mm ³ 204 volumes eyes closed	Matlab, DPABI Confound regression - Linear trend - GSR: CSF, WM, global Motion scrubbing - Mean FD > 0.2 mm	SCA from hippocampi Pearson correlation	FC ↗ WMH left hippocampus and right inf. orbital and inf. temporal gyrus
Healthy participants						
[79]	76 healthy participants	Mixture model [80]	GE Signa, 1.5 T TR 2000 ms, TE 40 ms □ × □ × 24, □ × □ × 5 mm ³ 240 volumes [eyes]	REST Confound regression - Head motion parameters - GSR: CSF, WM, global Motion scrubbing - > 58 outlier volumes (> 1.5 mm/1.5°)	PCC from ext. template SCA to define DMN Pearson correlation	No association between WMH load and FC Episodic memory ↗ medial PFC–left inferior parietal cortex FC in patients with low grey matter volume

Table 2 Summary of included articles analysing resting-state functional connectivity in healthy participants or patients without vascular cognitive impairment. We report imaging and clinical characteristics of patients included in each study, key steps in the acquisition and pre-processing of BOLD data, analysis of functional connectivity, and FC patterns found to be associated with CSVD. Descriptive statistics as extracted from articles are reported as range (min–max) and/or mean \pm standard deviation. Missing information is indicated by empty brackets (□). Reported are clinical characteristics of patients included in each study, details about the quantification of white matter hyperintensities, key steps in the analysis of functional connectivity, and FC patterns found to be associated with CSVD. Arrows indicate increased (↑) or reduced (↓) values, as well as positive (↗) and negative (↘) associations (*Continued*)

Reference	Participants	Quantification of WMH load	rs-fMRI acquisition parameters	BOLD pre-processing	FC analysis	FC patterns associated with CSVD
[81]	127 healthy (Harvard Ageing Brain Study)	Fazekas 0–1 vs. 2–3	Siemens Trio, 3 T, 12-channel head coil TR 3000 ms, TE 30 ms 72 × 72 × □, 3 × 3 × 3 mm ³ 124 volumes eyes open	SPM 8 Confound regression - Realignment params + derivatives - GSR; WM, CSF, global Motion scrubbing - Mean FD > 0.15 mm - ≥ 20 outlier volumes (> 0.75 mm/1.5°)	PCC and medial PFC from external DMN template Partial Pearson correlation Probabilistic tractography	↓ Association between PCC-medial PFC FC and mean diffusivity in cingulum bundle
[82]	186 clinically healthy (Harvard Ageing Brain Study)	Automated fuzzy-connected algorithm [70]	Siemens Trio, 3 T, 12-channel head coil TR 3000 ms, TE 30 ms 72 × 72 × 47, 3 × 3 × 3 mm ³ 2 × 124 volumes eyes open	SPM 8 Confound regression - 12 motion parameters Motion scrubbing - 'mean movement' > 0.2 mm - > 20 outlier volumes (> 0.75 mm/1.5°)	Template-based rotation to define DMN and FPCN Pearson correlation	No association between WMH load and FC
[83]	51 healthy participants	SPM Lesion Segmentation Tool [76]	Phillips Ingenia, 3 T TR 2600 ms, TE 35 ms 128 × 128 × 35, 1.8 × 1.8 × 4 mm ³ 125 volumes, [eyes]	REST, GIFT [Confound regression] [Motion scrubbing]	ICA to define DMN, SN, FPN, VN	FC in DMN ↗ WMH in the mediotemporal complex FC in SN ↗ WMH in the right S1 and sup./inf. parietal cortex
[84]	1584 healthy participants (Rotterdam Study)	Tract-specific WMH load [85]	GE Signa, 1.5 T TR 2900 ms, TE 60 ms 64 × 64 × 31, 3.3 × 3.3 × 3.3 mm ³ 160 volumes, eyes open	FSL Confound regression - Low-frequency drifts - Motion components - ICA Motion scrubbing - Max FD > 0.5 mm, abs. motion > 3 mm	Desikan–Killiany parcellation Pearson correlation Probabilistic tractography	FC ↘ WMH both tract-specific and global
[86]	145 healthy participants	SPM Lesion Segmentation Tool [76]	GE MR750, 3 T TR 1500 ms, TE 27 ms 64 × 64 × 29, 3.75 × 3.75 × 4 mm ³ 162 volumes eyes open	FSL Confound regression - GSR; CSF, WM Motion scrubbing - FD > 0.5 mm	ICA to define DMN, SMN, FPCN Pearson correlation	No association between WMH load and FC

Table 2 Summary of included articles analysing resting-state functional connectivity in healthy participants or patients without vascular cognitive impairment. We report imaging and clinical characteristics of patients included in each study, key steps in the acquisition and pre-processing of BOLD data, analysis of functional connectivity, and FC patterns found to be associated with CSVD. Descriptive statistics as extracted from articles are reported as range (min–max) and/or mean \pm standard deviation. Missing information is indicated by empty brackets (□). Reported are clinical characteristics of patients included in each study, details about the quantification of white matter hyperintensities, key steps in the analysis of functional connectivity, and FC patterns found to be associated with CSVD. Arrows indicate increased (↑) or reduced (↓) values, as well as positive (↗) and negative (↘) associations (*Continued*)

Reference	Participants	Quantification of WMH load	rs-fMRI acquisition parameters	BOLD pre-processing	FC analysis	FC patterns associated with CSVD
[87]	69 healthy participants	Coarse-to-fine in-house developed mathematical morphology method [88]	Phillips Achieva, 3 T TR 2050 ms, TE 25 ms 64 × 64 × 47, 3.2 × 3.2 × 3.2 mm ³ 210 volumes eyes open	CONN Confound regression - 6 motion parameters - GSR, WM, CSF [Motion scrubbing]	AAL atlas, DTI atlas Whole-brain SCA Intrinsic connectivity contrast	FC in the left cuneus and right sup. occipital cortex ↗ WMH in the right ant. corona radiata FC in the left superior occipital cortex ↗ WMH in the right superior corona radiata
[67]	400 healthy participants (Baltimore Longitudinal Study of Aging)	Multimodal supervised classification algorithm [89]	Phillips Achieva, 3 T TR 2000 ms, TE 30 ms [matrix], 3 × 3 × 3 mm ³ 180 volumes [eyes]	Confound regression - 24 motion parameters - GSR, global, WM, CSF Motion scrubbing - summary motion value' > 0.2 mm - Volume censoring (FD > 0.5 mm, < 5 min)	Geodesic graph-based segmentation Regional homogeneity Sparse connectivity patterns	Pattern of advanced brain ageing characterised by both increased WMH burden and reduced FC compared to resilient agers
[66]	11 healthy participants	Automated regression algorithm [90] using a Hidden Markov Random Field with Expectation Maximization [91]	Siemens Trio, 3 T TR 2000 ms, TE 27 ms 92 × 92 × 43, 2.5 × 2.5 × 3 mm ³ 240 volumes eyes closed	SPM12 Confound regression - Linear/quadratic, 18 motion parameters - GSR, CSF, WM Motion scrubbing -> 3 mm max, > 3° max -> 24 spikes (FD > 1 mm)	Brainetome atlas (228) Graph theory to define DMN Pearson correlation	No association between WMH load and DMN FC trajectories
[92]	562 healthy participants	SPM Lesion Segmentation Tool [76]	Phillips Achieva, 3 T TR 2000 ms, TE 20 ms 112 × 112 × 37, 2 × 2 × 3 mm ³ [volumes], [eyes]	[Confound regression] [Motion scrubbing] Mean FD as covariate in analysis	Desikan–Killiany parcellation FC measure not specified	No association between WMH load and FC
[93]	182 participants (UK Biobank)	BIANCA with manual correction [94]	Siemens Skyra, 3 T TR 735 ms, TE 39 ms 88 × 88 × 64, 2.4 × 2.4 × 2.4 mm ³ 490 volumes, [eyes]	FMRIB (FSL), ICA-FIX Confound regression - ICA [Motion scrubbing]	ICA, AAL atlas Pearson correlation Degree centrality	FC ↗ WMH in right orbitofrontal cortex

Table 2 Summary of included articles analysing resting-state functional connectivity in healthy participants or patients without vascular cognitive impairment. We report imaging and clinical characteristics of patients included in each study, key steps in the acquisition and pre-processing of BOLD data, analysis of functional connectivity, and FC patterns found to be associated with CSVD. Descriptive statistics as extracted from articles are reported as range (min–max) and/or mean \pm standard deviation. Missing information is indicated by empty brackets (□). Reported are clinical characteristics of patients included in each study, details about the quantification of white matter hyperintensities, key steps in the analysis of functional connectivity, and FC patterns found to be associated with CSVD. Arrows indicate increased (↑) or reduced (↓) values, as well as positive (↗) and negative (↘) associations (*Continued*)

Reference	Participants	Quantification of WMH load	rs-fMRI acquisition parameters	BOLD pre-processing	FC analysis	FC patterns associated with CSVD
[95]	250 healthy (Harvard Aging Brain Study)	Automated fuzzy-connected algorithm [70]	Siemens Trio, 3 T TR 3000 ms, TE 30 ms [matrix], 3 × 3 × 3 mm ³ 2 × 124 volumes, eyes open	SPM 8 Template-based rotation method [Confound regression] [Motion scrubbing]	Template-based rotation to define DMN, SMN, DMN, and FPCN Pearson correlation	Association between WMH load and FC not investigated FC in DMN ↘ risk of progression to MCI

especially in occipital and frontal areas, and WMH burden [87, 93], whereas in patients with late-life depression the pattern was more similar to the one seen in patients with CSVD [69, 71].

Assessment of cognitive impairment

In the majority of studies, cognitive testing on participants was performed and investigated in association with the extent of white matter disease and functional connectivity. In addition to scales covering the global level of cognitive functions and deficits (MMSE, MoCA, and CDR), impairments in specific cognitive domains were quantified by sub-scores of these global scales or specialised neuropsychological test batteries, operationalising, in particular, executive function, processing speed, and memory. Table 3 summarises key findings of individual studies in these different domains. Most studies were able to confirm known associations between CSVD and cognitive impairment on the one hand, and, albeit less robustly, between functional connectivity and cognitive impairment on the other hand. Only few articles, however, addressed the question of how structural white matter damage and functional connectivity interact to affect cognition. In one analysis of 127 clinically healthy participants of the Harvard Ageing Brain Study, it was shown that the extent of WMH-associated decoupling of structural and functional connectivity in the default mode network correlated with both executive function and memory [81]. Moreover, in a combined analysis of 140 healthy participants and 90 patients with both vascular and non-vascular cognitive impairment, the authors demonstrated that the association of higher WMH load with poorer executive function and memory scores was moderated by global functional connectivity in the FPCN and by local FC in the salience network [65].

Risk of bias and confounding

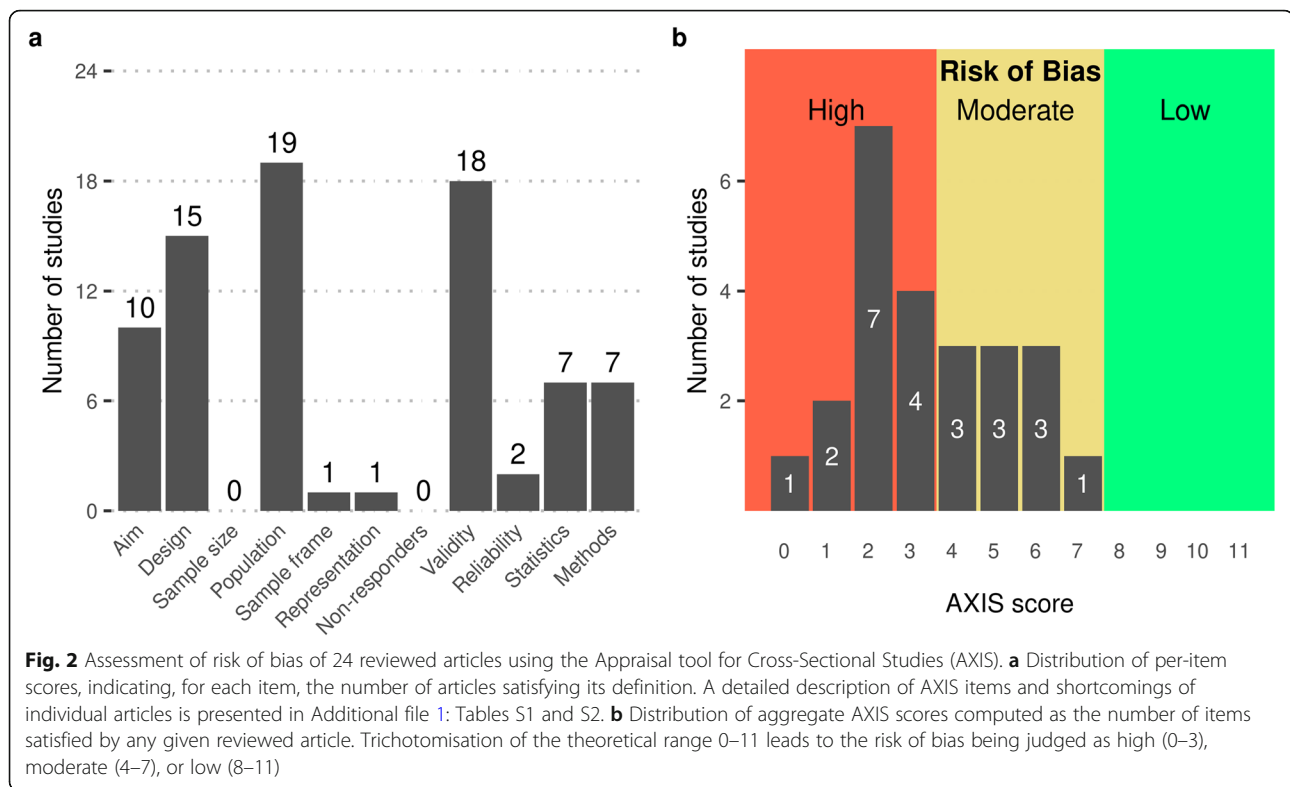
Risk of bias was assessed using the AXIS tool for all 24 studies recruiting patients with clinical CSVD. We did not formally assess the risk of bias in studies reporting results on FC and WMH in the context of conditions different from vascular cognitive impairment or in longitudinal studies. According to the AXIS tool, all studies thus assessed had an at least moderate risk of bias (10/24 moderate, 14/24 high). The distribution of assessments of individual quality items of the tool is depicted in Fig. 2 a. The overall aim or objective of the study (Item 1) was deemed unclear in 14 studies, often because of a lack of distinctions between exploratory and confirmatory, and causal and correlational approaches. In 9 cases, where aims included the inference of causal effects or were too broad to be assessed, a cross-sectional design was judged as inappropriate (Item 2). The sample size was not satisfactorily justified in any study. The

reference population (Item 4) was mostly adequately specified as patients with CSVD, qualified by lists of inclusion and exclusion criteria. In five studies, the definition of the target population was unclear or contradictory. All but one article reported results from single-centre studies that recruited a convenience sample from a clinical setting; in these cases, the sample frame (Item 5) was judged as inappropriate and the selection process (Item 6) as non-representative. The exceptions were an analysis of a formal clinical register [84, 99]. No article addressed non-responders. Risk factors and outcomes (Item 7) were mostly valid (see above); exceptions included one unvalidated method to quantify WMH load [87] and the use of global graph parameters such as efficiency and path length. Reliability of outcome measures (Item 9) was generally judged to be low given the poor reproducibility of FC estimates in the context of CSVD, except for studies who explicitly estimated reliability as part of the study design [31, 42]. There were two main problems with the statistical methods used: firstly, confusion of exploratory and confirmatory approaches (cf. Item 1) led to a lack of clearly specified hypotheses and thus to inappropriately controlled type-I error rates in the case of multiple testing; secondly, many papers employed multi-scale approaches, in which results from the first, often global, analyses informed hypotheses tested in later, often more local, analyses. It is known that this method can inflate the rate of false-positive findings if the entire analysis pipeline is not accounted for properly, for example in a bootstrap loop [100]. The quality of the description of methods varied considerably. No article provided links to the program code used in the analysis, but this was not required to satisfy Item 12. Specific shortcomings included incomplete reporting of MRI acquisition parameters, lack of description of structural image pre-processing, and lack of detail in the description of statistical methods, such as choice of covariates, method to determine of p -values, or correction for multiple testing. The distribution of aggregate AXIS scores is shown in Fig. 2b. Given that none of the included studies had a low risk of bias or was pre-registered, the overall risk of bias in the reviewed literature seems high.

Cardiovascular risk factors such as age, hypertension, diabetes mellitus, and dyslipidaemia are known to be associated with imaging markers of CSVD [101]. They also affect cerebrovascular reactivity and the circulatory auto-regulation in response to neuronal activity (*neurovascular coupling*) [29] and are thus potential confounders of the relation between WMH and BOLD-derived functional connectivity. Similarly, vasoactive medications, in particular antihypertensives, which are commonly prescribed to patients with CSVD as well as substances like nicotine or caffeine may alter neurovascular coupling

Table 3 Summary of reported associations between altered FC patterns in CSVD and cognitive ability. Arrows indicate positive (\nearrow) and negative (\searrow) associations

Cognitive domain	Reference	Instruments		
General	[47]	–	MMSE \nearrow FC between the left thalamus–left orbitofrontal lobe	
	[38]	–	MMSE \nearrow ReHo in the right angular gyrus and precuneus MoCA \nearrow ReHo in the bilateral angular gyrus, the right precuneus, medial/dorsolateral PFC, and supplementary motor area	
	[39]	–	MMSE \nearrow FC right precentral–right calcarine fissure, left posterior inferior parietal lobe–left Heschl, right posterior inferior parietal lobe–right dorsolateral PFC MMSE \searrow FC right posterior inferior parietal lobe–left Heschl, left intraparietal sulcus–right superior temporal gyrus MoCA \nearrow FC right posterior inferior parietal lobe–right anterior PFC, right posterior inferior parietal lobe–right dorsolateral PFC MoCA \searrow FC right posterior inferior parietal lobe–left Heschl, left intraparietal sulcus–right superior temporal gyrus	
	[53]	–	MoCA \nearrow small-worldness	
	[33]	–	MMSE \searrow parieto-occipital FC in patients with confluent WMH	
	Executive function	[35]	CERAD battery [96]	Phonemic fluency \nearrow FC in bilateral sup. parietal lobe, SMA, premotor cortex, MCC, and posterior superior frontal sulcus RT _{Stroop, neutral} \searrow FC in the bilateral premotor cortex, superior frontal sulcus, left inferior frontal sulcus, left SMA, left middle temporal sulcus, and right MCC RT _{Stroop, neutral} \nearrow FC in the inferior parietal lobe and cerebellar lobules Crus II, VIIb, and VIII RT _{TMT-A} \searrow FC in the bilateral premotor cortex, left posterior middle frontal gyrus, left inferior frontal sulcus, right superior parietal lobe, and left SMA RT _{Stroop, incongruent} \searrow FC in the left premotor cortex/posterior middle frontal gyrus RT _{Stroop, incongruent} \nearrow FC in the cerebellar regions VI, Crus I, and Crus II
[81]		Letter/category fluency, letter-number sequencing of the WAIS-III, Digit Span Backward of the WAIS revised (WAIS-R), Self-Ordered Pointing task, mod. Flanker task, and TMT A/B Confirmatory factor analysis [97]	Executive function \nearrow FC-SC decoupling in DMN	
[36]		Visuospatial/executive sub-score of MoCA	Executive function \nearrow FC in the right cingulate motor area	
[83]		Stroop test	Time interference index \nearrow FC in anterior DMN and SN	
[65]		TMT A/B, Stroop test Latent variables	Association (executive function \searrow WMH) attenuated in patients with high global FC in FPCN Associations (executive function \searrow WMH) and (memory \searrow WMH attenuated) in patients with high local FC in SN	
[51]		TMT-A/B, Stroop test	RT _{TMT-A} \searrow FC in FPCN in the right inferior parietal lobule RT _{TMT-A} \searrow FC between the dorsolateral PFC and DMN between bilateral PCC and right precuneus	
[43]		Semantic similarity test Stroop test	Mean FC \nearrow similarity index Stroop C score \nearrow path length, \searrow global efficiency	
Memory		[45]	Auditory Verbal Learning Test [AVLT] [98]	Delayed recall \searrow participation coefficient left superior parietal lobule Recognition \searrow characteristic path length
		[65]	AVLT, structural equation modelling	Memory \nearrow WML*global FC
		[52]	AVLT	FC \searrow long recall between right olfactory–right rectus; \searrow short recall between right olfactory–left pallidum FC \nearrow RT _{TMT-A} between right olfactory–left pallidum



[102]. Despite this, reporting of and adjustment for comorbidities and medication was poor in the reviewed studies. While information on the demographic variables age and sex was provided in all reviewed articles, only about half reported results of analyses adjusted for these factors. Nine articles gave details on cardiovascular risk factors, yet none attempted to control for their potential confounding effect. Effects of prescribed medication or caffeine intake were not considered.

Discussion

For this systematic review, we identified 44 articles published in the previous 10 years reporting on MRI-derived resting-state functional brain connectivity in patients with white matter hyperintensities of presumed vascular origin as a marker of cerebral small vessel disease. Based on patient characteristics and research objective, studies could be divided into three groups: (1) group comparisons of patients with clinically and/or radiologically manifest CSVD, often involving a control group of healthy participants or patients with CSVD at different levels of cognitive impairment; (2) cohort studies of clinically healthy individuals in which white matter hyperintensities are reported as one of several parameters, often with the aim of characterising structure–function relationships or patterns of brain ageing; (3) investigations of resting-state connectivity in clinical conditions not primarily related to vascular pathology, in which

measures of white matter disease were reported as covariates.

The overall median sample size of included studies was 68. There was a stark contrast in sample size between studies of patients with symptomatic CSVD (median 58, IQR 46–84, $n = 24$) and studies of clinically healthy participants (median 145, IQR 73–293, $n = 12$). Samples in studies focusing on non-vascular clinical conditions were of intermediate size (median 73, IQR 55–95, $n = 8$). These differences might be due to increased complexities associated with recruiting patients in a clinical context or the fact that some of the larger studies used data from comprehensive population-based research efforts, such as the Rotterdam Study [84, 103], the Harvard Brain Ageing Study [81, 82, 104], or the UK Biobank [93, 105].

Operationalisation of CSVD is study-context dependent

In addition to sample size, groups of studies also differed in their approaches to quantifying the severity of white matter disease. Clinically focused studies tended to rely on validated rating scales, such as the Fazekas or Wahlund scale, which assign an ordinal score based on the extent and distribution of white matter hyperintensities on T2-weighted MR imaging. A minority of studies considered the presence of lacunar infarcts as an additional marker for CSVD. The population-based studies of healthy participants, on the other hand, employed the

cumulative volume of WMH as a continuous measure of disease burden. Numerical lesion load has the advantage of providing better resolution of inter-individual differences in groups of mildly affected participants; in addition, it can be determined reasonably reliably using automatic or semi-automatic image processing methods, although some degree of manual post-processing was usually done in the studies reviewed here [106]. Brain atrophy as a structural marker of both CSVD and neurodegenerative disease is known to be associated with changes in intrinsic brain connectivity [107]; it was included in many of the population-based studies using either the total intracranial volume to normalise observed WMH loads or region-specific grey matter volume, such as can be obtained from voxel-based morphometry (VBM) or cortical thickness measurements. Although methods have been developed to segment perivascular spaces (PVS) and cerebral microbleeds in an automated fashion [108–114], none of the reviewed articles utilised enlarged PVS, and only one used microbleeds [49] as a marker of CSVD.

The variety of qualitative and quantitative analysis methods reflects the clinical heterogeneity of study populations comprising patients with CSVD at different stages of the disease. An attempt at standardising the assessment and reporting of imaging markers of CSVD was made in the STAndards for ReportIng Vascular changes on nEuroimaging (STRIVE) position paper [6]. However, despite being published in 2013, the definitions and recommendations outlined in the STRIVE were referenced in only six of the 33 reviewed papers published after 2013 [31, 50–52, 62, 108].

Functional connectivity methods reflect clinical heterogeneity

The analysis of recorded BOLD signals has not been standardised, with a broad variety of coupling measures and dimensionality reduction techniques being at the disposal of the researcher [20]. All reviewed studies used Pearson's correlation coefficient to quantify the synchrony between BOLD time series in different parts of the brain. No clear distinction between full and partial correlations was often made, thus making the interpretation of direct or indirect connectivities difficult [115]. Similarly, the handling and interpretation of negative correlations was rarely reported or discussed [116–118]. None of the included articles attempted to estimate directed [119–121] or time-varying functional connectivities [122–124], or to quantify patterns of synchronous activity involving more than two regions [125, 126]. Analytical approaches included whole-brain analyses (eigenvector centrality, connectivity density); the investigation of functional connectivities between region of interests, often components of well-defined intrinsic

resting-state networks, which were either derived from the data themselves (independent component analysis) or specified a priori by an external brain parcellation; and combinations of the two (seed-based correlation analysis).

Brain parcellations for the region-of-interest-based analyses were mostly based on anatomically defined atlases, such as the automatic anatomical labelling (AAL) atlas [127], the Desikan–Killiany parcellation [128], or the H-1024 random parcellation [129], which do not take into account the functional architecture of the brain. Only three very recent articles [31, 49, 66] used the multimodal brain parcellations of Power [130] or Schaefer [131], or the Brainnetome atlas [132], which have been shown to better respect the functional organisation of the brain [22]. In addition to interpreting changes in functional connectivity directly, a few studies attempted to summarise patterns of FC by measures of global network organisation using graph theory. These approaches have been instrumental in the study of complex brain networks and include parameters to reflect the notions of integration, such as efficiency or characteristic path length; segregation, such as clustering coefficients; or community structure, quantified by modularity scores and participation coefficients [9, 133, 134]. With the exception of community detection, however, these network parameters have been defined only for structural brain networks and lack validation for networks derived from functional connectivity [135].

Structure–function coupling shapes the impact of CSVD

The large-scale temporospatial organisation of neuronal activity in the brain is known to be supported and constrained by the anatomy of axonal projections that form structural connections between both adjacent and remote brain areas [136, 137]. This coupling between structure and function is particularly pronounced in the default mode network [138], possibly reflecting the long periods of time that the brain is engaged in inward-directed thought, memory formation and retrieval, or social estimation [139]. While the structural connectome thus contributes to maintaining stable neural activity patterns, it also means that normal functional connectivity is vulnerable to damage to white matter pathways as occurring in CSVD [140]. Most articles included in this review quantified the extent of white matter damage by using either neuroradiological rating scales or total lesion volume, as detailed above. Such global approaches are, however, not able to differentiate between lesions in functionally silent brain areas that can more easily be compensated by rerouting information through alternative redundant pathways, and lesions in functionally critical, strategic locations, where even spatially limited damage can be associated with substantial behavioural

sequelae. In the context of cognition, damage to subcortical nuclei and tracts with a high density of neuromodulatory projections such as the dorsomedial and anterior thalamic nuclei or the anterior limb of the internal capsule appears to be particularly consequential [24, 52, 87, 141]. Advanced diffusion-weighted structural imaging modalities allow the spatial mapping of fibre tracts and the quantification of tract-specific white matter lesion loads [142, 143]. In combination with resting-state BOLD imaging, this approach has been used to show that leukoaraiosis disrupts functional connectivity in a spatio-topological non-uniform way that is shaped by the anatomy of the brain's white matter scaffold [84]. The strongest association between tract-specific ischaemic damage and reduced FC was observed in the fronto-occipital fasciculus, which supports connectivity between the salience and frontoparietal control networks [144]. In addition to affecting functional connectivity directly, ischaemic white matter disease also seems to exert an indirect effect by modulating the coupling between structural and functional connectivity. Specifically, the association between mean diffusivity in the cingulum bundle and functional connectivity between the medial prefrontal and posterior cingulate cortices was significantly attenuated in patients with higher WMH burden, thus contributing to decoupling the anterior and posterior parts of the default mode network [81].

Both structural and functional connectomes share properties of complex networks, such as the presence of network communities, high-clustering with short path length (small-worldness), and hierarchical organisation [11, 145]. With cognition considered an emergent property of distributed neuronal activity in the brain [146, 147], understanding the behavioural sequelae of CSVD requires an understanding of how ischaemic lesions disturb not only specific fibre tracts and functional connections but also the global organisation of synchronous activity. Graph theoretical analyses have suggested that the global topology of functional brain networks in the presence of CSVD exhibits increased path length and modularity and reduced small-worldness that correlated with cognition [45, 53]. A similar effect was also observed in the structural networks of patients with CSVD and ischaemic stroke [13, 15, 148–150].

An intriguing open question is the differentiation between altered functional connectivity as a direct consequence of damage to the supporting fibre tracts, and compensatory changes. The latter are thought to contribute to maintaining normal cognitive function in the early stages of the disease [83]. Indeed, increased coupling between brain areas has repeatedly been reported in cognitively normal individual with white matter hyperintensities [78, 87, 93].

Resting-state FC informs an updated disconnection hypothesis

The association of white matter hyperintensities of presumed vascular origin with cognition has been extensively described [151–153], and indeed, cognitive impairment is one of the clinical hallmarks of manifest cerebral small vessel disease [154]. On the other hand, resting-state fMRI connectivity has been found useful in extracting neural correlates of cognitive function and mood disorders [155, 156]. Under normal physiological circumstances, patterns of coordinated activity within and between a small number of large-scale intrinsic brain networks have emerged as particularly relevant [146], including activation of the default mode network in brain states characterised by self-referential thought or rest that is anti-correlated with activation of the dorsal attention network; deactivation of the default mode network during focused attention on external stimuli [157]; and a modulating role of a frontoparietal control network with increased connectivity to the DMN as a correlate of working memory performance [158, 159]. Building upon these 'cornerstones' of functional connectivity under normal physiological circumstances, a disconnection hypothesis has been developed that postulates reduced DMN and FPCN connectivity, decoupling of neuronal activity along the anterior–posterior axis, and functional disconnection of the prefrontal cortex as neuronal correlates of cognitive impairment in CSVD [24]. This model is supported by several recent studies that reported decreased functional connectivity between the medial PFC and posterior components of the DMN in patients with CSVD [28, 44, 47], and observed an association with reaction times in the Stroop test [35]. A behaviorally relevant dissociation in functional resting-state fMRI activity and local connectivity was found between the anterior and posterior parts of the DMN with lower ReHo and ALFF values in the medial PFC and higher values in the precuneus and posterior cingulate cortex in patients with CSVD compared to healthy controls [38, 44]. Both increases and decreases of FC within the FPCN and DAN as well as their coupling with the DMN have been reported to be associated with CSVD [39, 46, 51], but the heterogeneity of these results and limited correlation with cognitive test scores makes it difficult to distinguish primary effects of disconnection from compensatory changes or sampling variability without physiological relevance.

In addition to these established networks, connectivity patterns of the salience network (SN) have recently been investigated, with increased SN-FPCN and SN-DMN couplings associated with small vessel disease [51]; additionally, increased connectivity within the SN in patients with CSVD was associated with worse performance in the Stroop interference test [83]. In patients with mild

cognitive impairment, the association between white matter disease and executive function was attenuated in the presence of increased local connectivity of the salience network [65]. The salience network includes the anterior insula, the dorsal anterior cingulate cortex, and subcortical components. Similar to the FPCN, it has a critical role in switching activity between different brain networks and has been implicated as a key component in network models of neuropsychiatric disorders [160–162]. Specifically, increased connectivity within the SN and altered SN-DMN and SN-FPCN coupling have been described in patients with Alzheimer's disease and mild cognitive impairment [163–165].

Community-dwelling adults with early CSVD often perform normally on neuropsychological tests and only report mild subjective cognitive deficits [166]. This pre-clinical stage has been linked to compensatory mechanisms especially in patients who benefit from a larger cognitive reserve [167, 168]. Three recent studies provide further evidence for this hypothesis, linking increased functional connectivity to frontal and temporal areas to ischaemic white matter lesion load in cognitively normal subjects [78, 83, 93].

Current knowledge is limited by the risk of bias, confounding, and methodological constraints

While it is possible to extract consistent themes from the reviewed articles that point toward physiologically relevant patterns of altered FC in the context of CSVD and cognitive impairment, the current literature is characterised by a high degree of heterogeneity of individual results. As discussed above, this may partly reflect variability in pre-processing and analytical approaches as well as heterogeneity in the clinical populations under investigation. However, given the absence of preregistered reports or high-quality multi-centre studies and the predominantly moderate-to-high risk of bias in individual studies, it must be assumed that selective reporting allowed the literature to be contaminated by a substantial number of false-positive findings, reflecting spurious associations and group differences. In addition, it is possible that reported results are confounded by the presence of other age-related pathology or neurodegenerative comorbidities, such as Alzheimer's disease [169], which were considered specifically in only a small minority of studies.

Comparison and synthesis of individual study findings is further hampered by differences in data cleaning techniques, which are known to influence functional connectivity estimates [170]. Two important dimensions of BOLD pre-processing relate to removal of the global signal from the whole brain or tissue type compartments, and handling of subjects or frames with high motion. Global signal regression is known to be effective at

mitigating the widespread inflation of connectivity estimates induced by subject motion, resulting in an elevated distance-dependence of residual motion artefacts [171]. Despite this theoretical prediction and the observation that GSR might improve associations between FC and behavioural measures [172], the use of GSR was not associated with specific patterns of altered connectivity or stronger relations with cognitive measures in the reviewed papers. Similarly, no clear effect of different motion scrubbing strategies, i.e. the censoring of subjects or individual volumes due to excessive average or frame-wise displacement, could be recognised. It seems likely that the myriad of unstandardised pre-processing choices is contributing to the heterogeneity of published results and that findings which have not been shown to be robust with respect to such choices should therefore be interpreted with great care.

Even ignoring potential biases inherent in study design and publication practice, the study of FC in the context of CSVD may be limited by more fundamental obstructions. One concern is that the reliability of estimating functional connectivity may be negatively affected by the presence of white matter lesions itself. Two of the reviewed studies reported results from repeated measurements on participants in longitudinal designs [31, 42]. Worryingly, in both cases, resting-state fMRI measures were found to be poorly reproducible, indicating a further need to evaluate their robustness as an imaging biomarker. In one case, this might have been a consequence, in part, of using a brain parcellation that does not respect the functional boundaries between brain areas, which is known to be damaging to network estimation [119]. However, the persistence of low reliability measures for a range of network characteristics across network densities and atlas resolutions, as well as the particularly poor reproducibility of functional network measures in patients with CSVD compared to controls, suggests more fundamental problems beyond the choice of parcellation. The finding of poor reproducibility of RSNs and graph metrics in CSVD contrasts with high reproducibility reported in healthy participants [173–176] and patients with stable multiple sclerosis [177–179]. It has been suggested that age and confounding age-related pathologies could be responsible for reduced reliability of functional connectivity estimates [180, 181]; however, specific methodological challenges arise in patients with cerebral small vessel disease as a consequence of microvascular pathology, that are absent in other conditions.

As a measure of synchronous brain activity, the interpretation of BOLD-derived functional connectivity is contingent upon an understanding of the relation between neuronal activity and local blood flow. This neurovascular coupling, however, is known to be altered in

normal ageing as well as the presence of ischaemic disease [102, 182, 183], and attributing differences in BOLD-derived measures of connectivity to either vascular or neuronal factors is therefore challenging [184]. More specifically, white matter lesions of presumed vascular origin are known to be associated with subcortical hypoperfusion [185], possibly reflecting observed rarefaction of the microcirculation in a mouse genetic model of CSVD [186]. The later stages of neurovascular coupling involve dynamic upregulation of regional blood flow mediated by increased CO₂ concentration in areas of increased neuronal activity [102]. This mechanism appears to be affected in the presence of CSVD as demonstrated by a diminished cerebrovascular response to hypercapnia in an early study involving 24 patients with leukoaraiosis [187], and an association between WMH load and sonographically assessed measures of pulsatility and dynamic autoregulation in a cohort of elderly patient with cardiovascular risk factors [188]. These findings are further complicated by differences in age-related changes in cerebrovascular reactivity between grey and white matter [189]. BOLD-derived functional connectivity is a function of BOLD activity in remote brain areas, and spatial variations in age- or disease-related changes in neurovascular coupling might therefore affect FC estimates in unpredictable ways [190]. A small study of 25 subjects with WMH found that while cardiovascular risk factors are associated with cerebrovascular reactivity, no such association was observed for resting-state functional connectivity in the default mode network [29]. One potentially testable hypothesis about the effects of impaired neurovascular coupling on functional connectivity estimates derives from the observation that BOLD-derived measures of synchronous brain activity are a composite of true coincident neuronal activation ('signal') and shared noise, where the latter tends to be more dominant for short-range connections [171]. Reduced 'signal' strength as a consequence of a lower vascular response would therefore be expected to result in weaker and less precise FC estimates, especially in long-range connections.

Limitations

While being comprehensive in our inclusion of primary research articles from electronic databases and other sources, we cannot exclude the possibility that additional findings from the grey literature, such as blogs or unpublished conference abstracts, have not been covered by this review. In order to keep the scope of the work focused, we have not included reports of task-based connectivity or resting-state connectivity derived from electrophysiological recordings. Findings obtained using these alternative paradigms and modalities might lend further support to the themes of disturbed connectivity

patterns outlined above. This review attempted a qualitative synthesis of the recent literature; the heterogeneity of study designs and populations did not permit the extraction and quantitative analysis of numerical effect estimates beyond sample size and age of participants. From a meta-analytical perspective, it can be noted, however, that all studies of patients with clinically manifest CSVD report significant FC alterations, while that is the case for only 30% of the population-based studies despite larger sample sizes. This discrepancy could reflect larger effect sizes in clinically preselected patients or indicate selective reporting in the sense of publication bias [191].

For conciseness, we have concentrated our attention on cognitive impairment as one of the main clinical sequelae of CSVD. Associations of altered patterns of functional connectivity with depressive symptoms, apathy, or gait imbalance were rarely reported and have not systemically been explored here. As an entry point to the recent literature, we note that abnormal functional coupling has been observed as a correlate of late-life depression in the context of the vascular depression hypothesis [192–195]; while apathy has been investigated using resting-state fMRI in various clinical contexts [196–198], results on gait disorders are scarce [34, 199]. Functional connectivity does not seem to interact with race or socio-economic status as possible contributing factors to neurodegeneration [200].

Conclusion

The large number of recent studies investigating resting-state fMRI connectivity in the presence of cerebral small vessel disease reflects an active ongoing interest to understand the interplay between structural brain damage, associated changes in the spatiotemporal organisation of neural activity, and clinical sequelae. The literature documents accumulating evidence for a network disruption model underlying cognitive impairment in CSVD that is characterised by disordered connectivity patterns in the DMN and FPCN and a decoupling of neuronal activity along the anterior–posterior axis, mediated by structural damage to long association tracts and cortico-subcortical connections. In addition, evidence is emerging that altered connectivity of the salience network might be a novel neuronal correlate of cognitive deficits in patients with CSVD.

The synthesis of population-based studies involving healthy participants with low white matter disease burden and clinical studies recruiting patients with manifest CSVD suggests a pattern of increased functional connectivity in various frontal and temporal brain areas consistent with compensatory upregulation at low white matter disease burden in the early stages of the disease, and dysfunctional patterns of functional connectivity

among distributed brain networks in more severely affected patients, possibly reflecting a break-down of compensatory mechanisms as the disease progresses and cognitive symptoms develop.

Further research is needed to address the problem of poor reproducibility of resting-state functional brain networks in patients with CSVD and to establish interacting effects of white matter damage of presumed vascular origin and functional reorganisation on cognition in preregistered, sufficiently powered, longitudinal studies. We expect particularly useful insights from multimodal investigations that combine resting-state and task functional MRI with electrophysiological recordings or metabolic imaging to improve temporal resolution and infer cellular processes relating to pathology.

Abbreviations

AAL: Automatic anatomical labelling; ACC: Anterior cingulate cortex; AD: Alzheimer's disease; AFNI: Analysis of Functional NeuroImages; ALFF: Amplitude of low-frequency fluctuations; AN: Auditory network; ANTs: Advanced Normalisation Tools; AROMA: Automatic Removal of Motion Artifacts; AVLT: Auditory verbal learning test; AXIS: Appraisal tool for Cross-Sectional Studies; BRAMILA: BRAin and MInd LAB; CADASIL: Cerebral autosomal dominant arteriopathy with subcortical infarcts and leukoencephalopathy; CDR: Clinical Dementia Rating scale; CERA D: Consortium to Establish a Registry for Alzheimer's Disease; CN: Cognitively normal; compCor: Component-based noise correction; CONN: Functional connectivity toolbox; CSF: Cerebrospinal fluid; CSVD: Cerebral small vessel disease; DAN: Dorsal attention network; DARTEL: Diffeomorphic Anatomical Registration using Exponentiated Lie algebra; DMN: Default mode network; DPABI: Data Processing & Analysis for Brain Imaging; DPARSF: Data Processing Assistant for Resting-State fMRI; DTI: Diffusion tensor imaging; EEG: Electroencephalography; fALFF: Fractional ALFF; FC: Functional connectivity; FD: Framewise displacement; FLAIR: Fluid-attenuated inversion recovery; FPCN: Frontoparietal control network; FSL: Functional Magnetic Resonance Imaging of the Brain Software Library; GIFT: Group ICA Of fMRI Toolbox; GRET NA: GRaph thEoreticAl Network Analysis; GSR: Global Signal Regression; HC: Healthy control; ICA: Independent component analysis; MCC: Middle cingulate cortex; MCI: Mild cognitive impairment; MMSE: Mini Mental State Exam; MoCA: Montreal Cognitive Assessment; MRI: Magnetic resonance imaging; NBS: Network-based statistics; PET: Positron emission tomography; PCC: Posterior cingulate cortex; PFC: Prefrontal cortex; PiB: Pittsburgh compound B; PRISMA: Preferred Reporting Items for Systematic Reviews and Meta-Analysis; ReHo: Regional homogeneity; REST: REsting State fMRI data analysis Toolkit; ROI: Region of interest; RSN: Resting-state network; RT: Reaction time; SC: Structural connectivity; SCA: Seed-based connectivity analysis; SMA: Supplementary motor area; SMN: Somatomotor network; SN: Salience network; SPM: Statistical Parametric Mapping; STRIVE: STandards for Reporting Vascular changes on nEuroimaging; SVaD: Subcortical vascular dementia; svMCI: Subcortical vascular MCI; T: Tesla; TE: Echo time; THA LAC: Thalamus lacune; TMT: Trail making test; TR: Repetition time; VBM: Voxel-based morphometry; VN: Visual network; WAIS: Wechsler Adult Intelligence Scale; WM: White matter; WWMH: White matter hyperintensity

Supplementary Information

Supplementary information accompanies this paper at <https://doi.org/10.1186/s12916-021-01962-1>.

Additional file 1: Search strategy. Detailed description of search parameters to identify relevant literature. Risk of bias assessment. Supplementary methods and results relating to the assessment of bias in individual studies. **Table S1.** Description of items used to score risk of bias. **Table S2.** Results of risk-of-bias assessments using the AXIS tool.

Acknowledgements

Not applicable

Authors' contributions

MS searched the literature, screened articles, extracted metadata and key results, and wrote a first version of the manuscript. CM revised the manuscript for critical intellectual content. BC secured funding and revised the manuscript for critical intellectual content. GT conceptualised the study, secured funding, and revised the manuscript for critical intellectual content. ES conceptualised the study, validated the inclusion and exclusion of articles, extracted metadata and key results, performed risk-of-bias assessment, synthesised findings, wrote the manuscript, and created tables and visualisations. The authors read and approved the final manuscript.

Funding

This work was supported by a grant from the German Research Foundation (Deutsche Forschungsgemeinschaft, DFG), Sonderforschungsbereich (SFB) 936, Project C2 (MS, GT, BC, ES). Open Access funding enabled and organized by Projekt DEAL.

Availability of data and materials

All data generated or analysed during this study are included in this published article and its supplementary information files.

Declarations

Ethics approval and consent to participate

No ethical approval or consent to participate was necessary for the presented study.

Consent for publication

Not applicable.

Competing interests

The authors declare that they have no competing interests.

Author details

¹Department of Neurology, University Medical Centre Hamburg-Eppendorf, Hamburg, Germany. ²Department of Computational Neuroscience, University Medical Centre Hamburg-Eppendorf, Hamburg, Germany.

Received: 9 March 2021 Accepted: 17 March 2021

Published online: 05 May 2021

References

- Wardlaw JM, Smith C, Dichgans M. Mechanisms of sporadic cerebral small vessel disease: insights from neuroimaging. *Lancet Neurol*. 2013;12:483–97. [https://doi.org/10.1016/S1474-4422\(13\)70060-7](https://doi.org/10.1016/S1474-4422(13)70060-7).
- Rensma SP, van Sloten TT, Launer LJ, Stehouwer CDA. Cerebral small vessel disease and risk of incident stroke, dementia and depression, and all-cause mortality: a systematic review and meta-analysis. *Neurosci Biobehav Rev*. 2018;90:164–73.
- Hu HY, Ou YN, Shen XN, Qu Y, Ma YH, Wang ZT, et al. White matter hyperintensities and risks of cognitive impairment and dementia: a systematic review and meta-analysis of 36 prospective studies. *Neurosci Biobehav Rev*. 2021;120:16–27.
- Feigin VL, Lawes CMM, Bennett DA, Anderson CS. Stroke epidemiology: a review of population-based studies of incidence, prevalence, and case-fatality in the late 20th century. *Lancet Neurol*. 2003;2:43–53.
- Fitzpatrick AL, Kuller LH, Ives DG, Lopez OL, Jagust W, Breitner JCS, et al. Incidence and prevalence of dementia in the cardiovascular health study. *J Am Geriatr Soc*. 2004;52:195–204. <https://doi.org/10.1111/j.1532-5415.2004.52058.x>.
- Wardlaw JM, Smith EE, Biessels GJ, Cordonnier C, Fazekas F, Frayne R, et al. Neuroimaging standards for research into small vessel disease and its contribution to ageing and neurodegeneration. *Lancet Neurol*. 2013;12:822–38. [https://doi.org/10.1016/S1474-4422\(13\)70124-8](https://doi.org/10.1016/S1474-4422(13)70124-8).
- Veldsman M, Kindalova P, Husain M, Kosmidis I, Nichols TE, Nichols E, et al. Spatial distribution and cognitive impact of cerebrovascular risk-related white matter hyperintensities. *BioRxiv*. 2020;28:2020.06.12.147934. <https://doi.org/10.1101/2020.06.12.147934>.

8. Cox SR, Lyall DM, Ritchie SJ, Bastin ME, Harris MA, Buchanan CR, et al. Associations between vascular risk factors and brain MRI indices in UK Biobank. *Eur Heart J*. 2019;40:2290–9. <https://doi.org/10.1093/eurheartj/ehz100>.
9. van den Heuvel MP, Sporns O. A cross-disorder connectome landscape of brain dysconnectivity. *Nat Rev Neurosci*. 2019;20:435–46. <https://doi.org/10.1038/s41583-019-0177-6>.
10. Fornito A, Zalesky A, Breakspear M. The connectomics of brain disorders. *Nat Rev Neurosci*. 2015;16:159–72. <https://doi.org/10.1038/nrn3901>.
11. Bassett DS, Sporns O. Network neuroscience. *Nat Neurosci*. 2017;20:353–64.
12. Rubinov M, Bullmore E. Fledgling pathoconnectomics of psychiatric disorders. *Trends Cogn Sci*. 2013;17:641–7. <https://doi.org/10.1016/j.tics.2013.10.007>.
13. Lawrence AJ, Chung AW, Morris RG, Markus HS, Barrick TR. Structural network efficiency is associated with cognitive impairment in small-vessel disease. *Neurology*. 2014;83:304–11. <https://doi.org/10.1212/WNL.0000000000000612>.
14. Tuladhar AM, Van Uden IWM, Rutten-Jacobs LCA, Lawrence A, Van Der Holst H, Van Norden A, et al. Structural network efficiency predicts conversion to dementia. *Neurology*. 2016;86:1112–9. <https://doi.org/10.1212/WNL.0000000000002502>.
15. Shen J, Tozer DJ, Markus HS, Tay J. Network efficiency mediates the relationship between vascular burden and cognitive impairment: a diffusion tensor imaging study in UK Biobank. *Stroke*. 2020;1682–9. <https://doi.org/10.1161/STROKEAHA.119.028587>.
16. Frey BM, Petersen M, Schlemm E, Mayer C, Hanning U, Engelke K, et al. White matter integrity and structural brain network topology in cerebral small vessel disease: the Hamburg city health study. *Hum Brain Mapp*. 2020; hbm.25301. doi:<https://doi.org/10.1002/hbm.25301>.
17. Gouw AA, Seewann A, Van Der Flier WM, Barkhof F, Rozemuller AM, Scheltens P, et al. Heterogeneity of small vessel disease: a systematic review of MRI and histopathology correlations. *J Neurol Neurosurg Psychiatry*. 2011; 82:126–35. <https://doi.org/10.1136/jnnp.2009.204685>.
18. Stephan BC, Matthews FE, Khaw K-T, Dufouil C, Brayne C. Beyond mild cognitive impairment: vascular cognitive impairment, no dementia (VCIND). *Alzheimers Res Ther*. 2009;1:4. <https://doi.org/10.1186/alzrt4>.
19. Hermann P, Romero C, Schmidt C, Reis C, Zerr I. CSF biomarkers and neuropsychological profiles in patients with cerebral small-vessel disease. *PLoS One*. 2014;9:e105000. <https://doi.org/10.1371/journal.pone.0105000>.
20. Wang HE, Bénar CG, Quilichini PP, Friston KJ, Jirsa VK, Bernard C. A systematic framework for functional connectivity measures. *Front Neurosci*. 2014;405 <https://doi.org/10.3389/fnins.2014.00405>.
21. van den Heuvel MP, Hulshoff Pol HE. Exploring the brain network: a review on resting-state fMRI functional connectivity. *Eur Neuropsychopharmacol*. 2010;20:519–34. <https://doi.org/10.1016/j.euroneuro.2010.03.008>.
22. Yeo BT, Krienen FM, Sepulcre J, Sabuncu MR, Lashkari D, Hollinshead M, et al. The organization of the human cerebral cortex estimated by intrinsic functional connectivity. *J Neurophysiol*. 2011;106:1125–65.
23. Ter Telgte A, Van Leijssen EMC, Wiegertjes K, Klijn CJM, Tuladhar AM, De Leeuw FE. Cerebral small vessel disease: from a focal to a global perspective. *Nat Rev Neurol*. 2018;14:387–98. <https://doi.org/10.1038/s41582-018-0014-y>.
24. Dey AK, Stamenova V, Turner G, Black SE, Levine B. Pathoconnectomics of cognitive impairment in small vessel disease: a systematic review. *Alzheimers Dement*. 2016;12:831–45. <https://doi.org/10.1016/j.jalz.2016.01.007>.
25. Liberati A, Altman DG, Tetzlaff J, Mulrow C, Gotzsche PC, Ioannidis JPA, et al. The PRISMA statement for reporting systematic reviews and meta-analyses of studies that evaluate health care interventions: explanation and elaboration. *J Clin Epidemiol*. 2009;62:e1–34. <https://doi.org/10.1016/j.jclinepi.2009.06.006>.
26. Downes MJ, Brennan ML, Williams HC, Dean RS. Development of a critical appraisal tool to assess the quality of cross-sectional studies (AXIS). *BMJ Open*. 2016;6:e011458. <https://doi.org/10.1136/bmjopen-2016-011458>.
27. Ma LL, Wang YY, Yang ZH, Huang D, Weng H, Zeng XT. Methodological quality (risk of bias) assessment tools for primary and secondary medical studies: what are they and which is better? *Military Med Res*. 2020;7:1–11. <https://doi.org/10.1186/s40779-020-00238-8>.
28. Sun Y, Qin L, Zhou Y, Xu Q, Qian L, Tao J, et al. Abnormal functional connectivity in patients with vascular cognitive impairment, no dementia: a resting-state functional magnetic resonance imaging study. *Behav Brain Res*. 2011;223:388–94.
29. Tchistiakova E, Crane DE, Mikulis DJ, Anderson ND, Greenwood CE, Black SE, et al. Vascular risk factor burden correlates with cerebrovascular reactivity but not resting state coactivation in the default mode network. *J Magn Reson Imaging*. 2015;42(5):1369–76.
30. Li R, Lai Y, Zhang Y, Yao L, Wu X. Classification of cognitive level of patients with leukoaraiosis on the basis of linear and non-linear functional connectivity. *Front Neurol*. 2017;8(2):12.
31. Gesierich B, Tuladhar AM, ter Telgte A, Wiegertjes K, Konieczny MJ, Finsterwalder S, et al. Alterations and test–retest reliability of functional connectivity network measures in cerebral small vessel disease. *Hum Brain Mapp*. 2020;41:2629–41. <https://doi.org/10.1002/hbm.24967>.
32. Wahlund LO, Barkhof F, Fazekas F, Bronge L, Augustin M, Sjögren M, et al. A new rating scale for age-related white matter changes applicable to MRI and CT. *Stroke*. 2001;32:1318–22.
33. Kumar D, Vipin A, Wong B, Ng KP, Kandiah N. Differential effects of confluent and nonconfluent white matter hyperintensities on functional connectivity in mild cognitive impairment. *Brain Connect*. 2020;10:547–54. <https://doi.org/10.1089/brain.2020.0784>.
34. Zhou X, Zhang C, Li L, Zhang Y, Zhang W, Yin W, et al. Altered brain function in cerebral small vessel disease patients with gait disorders: a resting-state functional MRI study. *Front Aging Neurosci*. 2020;12 <https://doi.org/10.3389/fnagi.2020.00234>.
35. Schaefer A, Quinque EM, Kipping JA, Arélin K, Roggenhofer E, Frisch S, et al. Early small vessel disease affects frontoparietal and cerebellar hubs in close correlation with clinical symptoms - a resting-state fMRI study. *J Cereb Blood Flow Metab*. 2014;7(7):1091–5.
36. Wu X, Lai Y, Zhang Y, Yao L, Wen X. Breakdown of sensorimotor network communication in leukoaraiosis. *Neurodegener Dis*. 2015;15:322–30.
37. Cheng R, Qi H, Liu Y, Zhao S, Li C, Liu C, et al. Abnormal amplitude of low-frequency fluctuations and functional connectivity of resting-state functional magnetic resonance imaging in patients with leukoaraiosis. *Brain Behav*. 2017;7(6):e00714.
38. Ding X, Ding J, Hua B, Xiong X, Xiao L, Peng F, et al. Abnormal cortical functional activity in patients with ischemic white matter lesions: a resting-state functional magnetic resonance imaging study. *Neurosci Lett*. 2017;644: 10–17.
39. Ding J-RR, Ding X, Hua B, Xiong X, Wen Y, Ding Z, et al. Altered connectivity patterns among resting state networks in patients with ischemic white matter lesions. *Brain Imaging Behav*. 2018;12:1239–50.
40. Friston KJ, Williams S, Howard R, Frackowiak RSJ, Turner R. Movement-related effects in fMRI time-series. *Magn Reson Med*. 1996;35:346–55.
41. Zalesky A, Fornito A, Bullmore ET. Network-based statistic: identifying differences in brain networks. *Neuroimage*. 2010;53:1197–207.
42. Lawrence AJ, Tozer DJ, Stamatakis EA, Markus HS. A comparison of functional and tractography based networks in cerebral small vessel disease. *NeuroImage Clin*. 2018;18:425–32. <https://doi.org/10.1016/j.nicl.2018.02.013>.
43. Zhu Y, Lu T, Xie C, Wang Q, Wang Y, Cao X, et al. Functional disorganization of small-world brain networks in patients with ischemic leukoaraiosis. *Front Aging Neurosci*. 2020;12 <https://doi.org/10.3389/fnagi.2020.00203>.
44. Yi L, Wang J, Jia L, Zhao Z, Lu J, Li K, et al. Structural and functional changes in subcortical vascular mild cognitive impairment: a combined voxel-based morphometry and resting-state fMRI study. *PLoS One*. 2012;7:e44758. <https://doi.org/10.1371/journal.pone.0044758>.
45. Yi LY, Liang X, Liu DM, Sun B, Ying S, Yang DB, et al. Disrupted topological organization of resting-state functional brain network in subcortical vascular mild cognitive impairment. *CNS Neurosci Ther*. 2015;21:846–54.
46. Kim HJ, Cha J, Lee JM, Shin JS, Jung NY, Kim YJ, et al. Distinct resting state network disruptions among Alzheimer's disease, subcortical vascular dementia, and mixed dementia patients. *J Alzheimers Dis*. 2016;50:709–18.
47. Zhou X, Hu X, Zhang C, Wang H, Zhu X, Xu L, et al. Aberrant functional connectivity and structural atrophy in subcortical vascular cognitive impairment: relationship with cognitive impairments. *Front Aging Neurosci*. 2016;8(14):8.
48. Chen H, Li Y, Liu Q, Shi Q, Wang J, Shen H, et al. Abnormal interactions of the salience network, central executive network, and default-mode network in patients with different cognitive impairment loads caused by leukoaraiosis. *Front Neural Circuits*. 2019;13 <https://doi.org/10.3389/fncl.2019.00042>.
49. Franzmeier N, Rubinski A, Neitzel J, Kim Y, Damm A, Na DL, et al. Functional connectivity associated with tau levels in ageing, Alzheimer's, and small vessel disease. *Brain*. 2019;142:1093–107. <https://doi.org/10.1093/brain/awz026>.

50. Liu R, Chen H, Qin R, Gu Y, Chen X, Zou J, et al. The altered reconfiguration pattern of brain modular architecture regulates cognitive function in cerebral small vessel disease. *Front Neurol*. 2019;324 <https://doi.org/10.3389/fneur.2019.00324>.
51. Liu R, Wu W, Ye Q, Gu Y, Zou J, Chen X, et al. Distinctive and pervasive alterations of functional brain networks in cerebral small vessel disease with and without cognitive impairment. *Dement Geriatr Cogn Disord*. 2019;47: 55–67. <https://doi.org/10.1159/000496455>.
52. Qin Y, Zhu W, Liu C, Wang Z, Zhu W. Functional brain connectome and its relation to mild cognitive impairment in cerebral small vessel disease patients with thalamus lacunes: a cross-sectional study. *Med (United States)*. 2019;98 <https://doi.org/10.1097/MD.00000000000017127>.
53. Wang J, Chen Y, Liang H, Niedermayer G, Chen H, Li Y, et al. The role of disturbed small-world networks in patients with white matter lesions and cognitive impairment revealed by resting state function magnetic resonance images (rs-fMRI). *Med Sci Monit*. 2019;25:341–56.
54. Shi Q, Chen H, Jia Q, Yuan Z, Wang J, Li Y, et al. Altered granger causal connectivity of resting-state neural networks in patients with leukoaraiosis-associated cognitive impairment—a cross-sectional study. *Front Neurol*. 2020;11 <https://doi.org/10.3389/fneur.2020.00457>.
55. Fazekas F, Barkhof F, Wahlund LO, Pantoni L, Erkinjuntti T, Scheltens P, et al. CT and MRI rating of white matter lesions. *Cerebrovasc Dis*. 2002;13(SUPPL. 2):31–6. <https://doi.org/10.1159/000049147>.
56. Fazekas F, Chawluk JB, Alavi A, Hurtig HI, Zimmerman RA. MR signal abnormalities at 1.5 T in Alzheimer's dementia and normal aging. *Am J Roentgenol*. 1987;149:351–6. <https://doi.org/10.2214/ajr.149.2.351>.
57. Andreescu C, Tudorascu DL, Butters MA, Tamburo E, Patel M, Price J, et al. Resting state functional connectivity and treatment response in late-life depression. *Psychiatry Res*. 2011;194:39–46. <https://doi.org/10.1016/j.psychres.2011.04.003>.
58. Román GC, Tatemichi TK, Erkinjuntti T, Cummings JL, Masdeu JC, Garcia JH, et al. Vascular dementia: diagnostic criteria for research studies: report of the NINDS-AIREN International Workshop. *Neurology*. 1993;43:250–60. <https://doi.org/10.1212/WNL.43.2.250>.
59. McKhann G, Drachman D, Folstein M, Katzman R, Price D, Stadlan EM. Clinical diagnosis of Alzheimer's disease: report of the NINCDS-ADRDA work group under the auspices of department of health and human services task force on Alzheimer's disease. *Neurology*. 1984;34:939–44. <https://doi.org/10.1212/wnl.34.7.939>.
60. Knopman DS, Boeve BF, Petersen RC. Essentials of the proper diagnoses of mild cognitive impairment, dementia, and major subtypes of dementia. In: *Mayo Clinic Proceedings*. Elsevier Ltd; 2003. p. 1290–1308. doi:<https://doi.org/10.4065/78.10.1290>.
61. Petersen RC, Caracciolo B, Brayne C, Gauthier S, Jelic V, Fratiglioni L. Mild cognitive impairment: a concept in evolution. *J Intern Med*. 2014;275:214–28. <https://doi.org/10.1111/joim.12190>.
62. Zhou Y, Yu F, Duong TQ. White matter lesion load is associated with resting state functional MRI activity and amyloid PET but not FDG in mild cognitive impairment and early Alzheimer's disease patients. *J Magn Reson Imaging*. 2015;41:102–9.
63. Franzmeier N, Caballero MAA, Taylor ANW, Simon-Vermot L, Buerger K, Ertl-Wagner B, et al. Resting-state global functional connectivity as a biomarker of cognitive reserve in mild cognitive impairment. *Brain Imaging Behav*. 2017;11:368–82.
64. Evans AC, Janke AL, Collins DL, Baillet S. Brain templates and atlases. *Neuroimage*. 2012;62:911–22.
65. Benson G, Hildebrandt A, Lange C, Schwarz C, Kobe T, Sommer W, et al. Functional connectivity in cognitive control networks mitigates the impact of white matter lesions in the elderly. *Alzheimers Res Ther*. 2018;10:109. <https://doi.org/10.1186/s13195-018-0434-3>.
66. Staffaroni AM, Brown JA, Casaleto KB, Elahi FM, Deng J, Neuhaus J, et al. The longitudinal trajectory of default mode network connectivity in healthy older adults varies as a function of age and is associated with changes in episodic memory and processing speed. *J Neurosci*. 2018;38:2809–17.
67. Eavani H, Habes M, Satterthwaite TD, An Y, Hsieh M-KK, Honnorat N, et al. Heterogeneity of structural and functional imaging patterns of advanced brain aging revealed via machine learning methods. *Neurobiol Aging*. 2018; 71:41–50. <https://doi.org/10.1016/j.neurobiolaging.2018.06.013>.
68. Jiang L, Zuo XN. Regional homogeneity: a multimodal, multiscale neuroimaging marker of the human connectome. *Neuroscientist*. 2016;22: 486–505.
69. Wu M, Andreescu C, Butters MA, Tamburo R, Reynolds CF, Aizenstein H. Default-mode network connectivity and white matter burden in late-life depression. *Psychiatry Res - Neuroimaging*. 2011;194:39–46. <https://doi.org/10.1016/j.psychres.2011.04.003>.
70. Wu M, Rosano C, Butters M, Whyte E, Nable M, Crooks R, et al. A fully automated method for quantifying and localizing white matter hyperintensities on MR images. *Psychiatry Res - Neuroimaging*. 2006;148: 133–42. <https://doi.org/10.1016/j.psychres.2006.09.003>.
71. Andreescu C, Tudorascu DL, Butters MA, Tamburo E, Patel M, Price J, et al. Resting state functional connectivity and treatment response in late-life depression. *Psychiatry Res - Neuroimaging*. 2013;214:313–21. <https://doi.org/10.1016/j.psychres.2013.08.007>.
72. Mikheev A, Nevsky G, Govindan S, Grossman R, Rusinek H. Fully automatic segmentation of the brain from T1-weighted MRI using Bridge Burner algorithm. *J Magn Reson Imaging*. 2008;27:1235–41. <https://doi.org/10.1002/jmri.21372>.
73. Suo C, Singh MF, Gates N, Wen W, Sachdev P, Brodaty H, et al. Therapeutically relevant structural and functional mechanisms triggered by physical and cognitive exercise. *Mol Psychiatry*. 2016;21:1633–42. <https://doi.org/10.1038/mp.2016.19>.
74. Wen W, Sachdev P. The topography of white matter hyperintensities on brain MRI in healthy 60- to 64-year-old individuals. *Neuroimage*. 2004;22: 144–54. <https://doi.org/10.1016/j.neuroimage.2003.12.027>.
75. Otsu N. Threshold selection method from gray-level histograms. *IEEE Trans Syst Man Cybern*. 1979;SMC-9:62–6.
76. Schmidt P, Gaser C, Arsic M, Buck D, Förschler A, Berthele A, et al. An automated tool for detection of FLAIR-hyperintense white-matter lesions in multiple sclerosis. *Neuroimage*. 2012;59:3774–83. <https://doi.org/10.1016/j.neuroimage.2011.11.032>.
77. Lyu H, Wang J, Xu J, Zheng H, Yang X, Lin S, et al. Structural and functional disruptions in subcortical vascular mild cognitive impairment with and without depressive symptoms. *Frontiers Media SA*; 2019. doi:<https://doi.org/10.3389/fnagi.2019.00241>.
78. Zhang XD, Zhao LR, Zhou JM, Su YY, Ke J, Cheng Y, et al. Altered hippocampal functional connectivity in primary Sjögren syndrome: a resting-state fMRI study. *Lupus*. 2020;29:446–54. <https://doi.org/10.1177/0961203320908936>.
79. He J, Carmichael O, Fletcher E, Singh B, Iosif A-MM, Martinez O, et al. Influence of functional connectivity and structural MRI measures on episodic memory. *Neurobiol Aging*. 2012;33:2612–20. <https://doi.org/10.1016/j.neurobiolaging.2011.12.029>.
80. DeCarli C, Massaro J, Harvey D, Hald J, Tullberg M, Au R, et al. Measures of brain morphology and infarction in the Framingham heart study: establishing what is normal. *Neurobiol Aging*. 2005;26:491–510. <https://doi.org/10.1016/j.neurobiolaging.2004.05.004>.
81. Reijmer YD, Schultz AP, Leemans A, O'Sullivan MJ, Guroi ME, Sperling R, et al. Decoupling of structural and functional brain connectivity in older adults with white matter hyperintensities. *Neuroimage*. 2015;117:222–9. <https://doi.org/10.1016/j.neuroimage.2015.05.054>.
82. Hedden T, Schultz AP, Rieckmann A, Mormino EC, Johnson KA, Sperling RA, et al. Multiple brain markers are linked to age-related variation in cognition. *Cereb Cortex*. 2016;26:1388–400. <https://doi.org/10.1093/cercor/bhu238>.
83. De Marco M, Manca R, Mitolo M, Venneri A. White matter hyperintensity load modulates brain morphometry and brain connectivity in healthy adults: a neuroplastic mechanism? *Neural Plast*. 2017;2017:10.
84. Langen CD, Zonneveld HI, White T, Huizinga W, Cremers LGM, de Groot M, et al. White matter lesions relate to tract-specific reductions in functional connectivity. *Neurobiol Aging*. 2017;51:97–103. <https://doi.org/10.1016/j.neurobiolaging.2016.12.004>.
85. de Boer R, Vrooman HA, van der Lijn F, Vernooij MW, Ikram MA, van der Lugt A, et al. White matter lesion extension to automatic brain tissue segmentation on MRI. *Neuroimage*. 2009;45:1151–61.
86. Madden DJ, Parks EL, Tallman CW, Boylan MA, Hoagey DA, Cocjin SB, et al. Sources of disconnection in neurocognitive aging: cerebral white-matter integrity, resting-state functional connectivity, and white-matter hyperintensity volume. *Neurobiol Aging*. 2017;54:199–213.
87. Shi L, Miao X, Lou W, Liu K, Abrigo J, Wong A, et al. The spatial associations of cerebral blood flow and spontaneous brain activities with white matter hyperintensities—an exploratory study using multimodal magnetic resonance imaging. *Front Neurol*. 2017. doi: <https://doi.org/10.3389/fneur.2017.00593>.

88. Shi L, Wang D, Liu S, Pu Y, Wang Y, Chu WCV, et al. Automated quantification of white matter lesion in magnetic resonance imaging of patients with acute infarction. *J Neurosci Methods*. 2013;213:138–46. <https://doi.org/10.1016/j.jneumeth.2012.12.014>.
89. Lao Z, Shen D, Liu D, Jawad AF, Melhem ER, Launer LJ, et al. Computer-assisted segmentation of white matter lesions in 3D MR images using support vector machine. *Acad Radiol*. 2008;15:300–13.
90. Dadar M, Pascoal TA, Manitsirikul S, Misquitta K, Fonov VS, Tartaglia MC, et al. Validation of a regression technique for segmentation of white matter hyperintensities in Alzheimer's disease. *IEEE Trans Med Imaging*. 2017;36:1758–68. <https://doi.org/10.1109/TMI.2017.2693978>.
91. Avants BB, Tustison NJ, Wu J, Cook PA, Gee JC. An open source multivariate framework for N-tissue segmentation with evaluation on public data. *Neuroinformatics*. 2011;9:381–400. <https://doi.org/10.1007/s12021-011-9109-y>.
92. Tsapanou A, Habeck C, Gazes Y, Razlighi Q, Sakhardande J, Stern Y, et al. Brain biomarkers and cognition across adulthood. *Hum Brain Mapp*. 2019;40:3832–42. <https://doi.org/10.1002/hbm.24634>.
93. Park BY, Byeon K, Lee MJ, Kim SH, Park H. The orbitofrontal cortex functionally links obesity and white matter hyperintensities. *Sci Rep*. 2020;10 <https://doi.org/10.1038/s41598-020-60054-x>.
94. Griffanti L, Zamboni G, Khan A, Li L, Bonifacio G, Sundaresan V, et al. BIANCA (Brain Intensity AbNormality Classification Algorithm): a new tool for automated segmentation of white matter hyperintensities. *Neuroimage*. 2016;141:191–205. <https://doi.org/10.1016/j.neuroimage.2016.07.018>.
95. Rabin JS, Neal TE, Nierle HE, Sikkes SAM, Buckley RF, Amariglio RE, et al. Multiple markers contribute to risk of progression from normal to mild cognitive impairment. *Neuroimage Clin*. 2020;28 <https://doi.org/10.1016/j.nicl.2020.102400>.
96. Fillenbaum GG, van Belle G, Morris JC, Mohs RC, Mirra SS, Davis PC, et al. Consortium to establish a registry for Alzheimer's disease (CERAD): the first twenty years. *Alzheimer's and Dementia*. 2008;4:96–109. <https://doi.org/10.1016/j.jalz.2007.08.005>.
97. Hedden T, Van Dijk KRA, Shire EH, Sperling RA, Johnson KA, Buckner RL. Failure to modulate attentional control in advanced aging linked to white matter pathology. *Cereb Cortex*. 2012;22:1038–51. <https://doi.org/10.1093/cercor/bhr172>.
98. Rey A. L'examen psychologique dans les cas d'encéphalopathie traumatique. *Arch Psychol*. 1941;28:215–285. doi:1943–03814-001.
99. Petersen RC, Aisen PS, Beckett LA, Donohue MC, Gamst AC, Harvey DJ, et al. Alzheimer's Disease Neuroimaging Initiative (ADNI): clinical characterization. *Neurology*. 2010;74:201–9. <https://doi.org/10.1212/WNL.0b013e3181cb3e25>.
100. Kriegeskorte N, Simmons WK, Bellgowan PS, Baker CI. Circular analysis in systems neuroscience: the dangers of double dipping. *Nat Neurosci*. 2009;12:535–40. <https://doi.org/10.1038/nn.2303>.
101. Van Dijk EJ, Breteler MMB, Schmidt R, Berger K, Nilsson LG, Oudkerk M, et al. The association between blood pressure, hypertension, and cerebral white matter lesions: cardiovascular determinants of dementia study. *Hypertension*. 2004;44(5):625–30.
102. D'Esposito M, Deouell LY, Gazzaley A. Alterations in the BOLD fMRI signal with ageing and disease: a challenge for neuroimaging. *Nat Rev Neurosci*. 2003;4:863–72. <https://doi.org/10.1038/nrn1246>.
103. Hofman A, Breteler MMB, Van Duijn CM, Krestin GP, Pols HA, Stricker BHC, et al. The Rotterdam study: objectives and design update. *Eur J Epidemiol*. 2007;22:819–29. <https://doi.org/10.1007/s10654-007-9199-x>.
104. Dagley A, LaPoint M, Huijbers W, Hedden T, McLaren DG, Chatwal JP, et al. Harvard aging brain study: dataset and accessibility. *Neuroimage*. 2017;144 Pt B:255–8. doi:<https://doi.org/10.1016/j.neuroimage.2015.03.069>.
105. Sudlow C, Gallacher J, Allen N, Beral V, Burton P, Danesh J, et al. UK biobank: an open access resource for identifying the causes of a wide range of complex diseases of middle and old age. *PLoS Med*. 2015;12:e1001779. <https://doi.org/10.1371/journal.pmed.1001779>.
106. Frey BM, Petersen M, Mayer C, Schulz M, Cheng B, Thomalla G. Characterization of white matter hyperintensities in large-scale MRI-studies. *Front Neurol*. 2019;238:16.
107. Lehmann M, Madison CM, Ghosh PM, Seeley WW, Mormino E, Greicius MD, et al. Intrinsic connectivity networks in healthy subjects explain clinical variability in Alzheimer's disease. *Proc Natl Acad Sci U S A*. 2013;110:11606–11. <https://doi.org/10.1073/pnas.1221536110>.
108. Park SH, Zong X, Gao Y, Lin W, Shen D. Segmentation of perivascular spaces in 7 T MR image using auto-context model with orientation-normalized features. *Neuroimage*. 2016;134:223–35.
109. Ballerini L, Booth T, Valdés Hernández M del C, Wiseman S, Lovreglio R, Muñoz Maniega S, et al. Computational quantification of brain perivascular space morphologies: associations with vascular risk factors and white matter hyperintensities. A study in the Lothian Birth Cohort 1936. *Neuroimage Clin*. 2020;25:102120. doi:<https://doi.org/10.1016/j.nicl.2019.102120>.
110. Dubost F, Yilmaz P, Adams H, Bortsova G, Ikram MA, Niessen W, et al. Enlarged perivascular spaces in brain MRI: automated quantification in four regions. *Neuroimage*. 2019;185:534–44.
111. Boespflug EL, Schwartz DL, Lahna D, Pollock J, Iliff JJ, Kaye JA, et al. MR imaging-based multimodal autoidentification of perivascular spaces (mMAPS): automated morphologic segmentation of enlarged perivascular spaces at clinical field strength. *Radiology*. 2018;286:632–42. <https://doi.org/10.1148/radiol.2017170205>.
112. Chen H, Yu L, Dou Q, Shi L, Mok VCT, Heng PA. Automatic detection of cerebral microbleeds via deep learning based 3D feature representation. In: Proceedings - International Symposium on Biomedical Imaging. New York: IEEE Computer Society; 2015. p. 764–7.
113. Seghier ML, Kolanko MA, Leff AP, Jäger HR, Gregoire SM, Werring DJ. Microbleed detection using automated segmentation (MIDAS): a new method applicable to standard clinical MR images. *PLoS One*. 2011;6 <https://doi.org/10.1371/journal.pone.0017547>.
114. Morrison MA, Payabvash S, Chen Y, Avadiappan S, Shah M, Zou X, et al. A user-guided tool for semi-automated cerebral microbleed detection and volume segmentation: evaluating vascular injury and data labelling for machine learning. *Neuroimage Clin*. 2018;20:498–505. <https://doi.org/10.1016/j.nicl.2018.08.002>.
115. Marrelec G, Krainik A, Duffau H, Pélégrini-Issac M, Lehéricy S, Doyon J, et al. Partial correlation for functional brain interactivity investigation in functional MRI. *Neuroimage*. 2006;32:228–37. <https://doi.org/10.1016/j.neuroimage.2005.12.057>.
116. Cole DM, Smith SM, Beckmann CF. Advances and pitfalls in the analysis and interpretation of resting-state fMRI data. *Front Syst Neurosci*. 2010;4 <https://doi.org/10.3389/fnsys.2010.00008>.
117. Fox MD, Zhang D, Snyder AZ, Raichle ME. The global signal and observed anticorrelated resting state brain networks. *J Neurophysiol*. 2009;101:3270–83. <https://doi.org/10.1152/jn.90777.2008>.
118. Murphy K, Birn RM, Handwerker DA, Jones TB, Bandettini PA. The impact of global signal regression on resting state correlations: are anti-correlated networks introduced? *Neuroimage*. 2009;44:893–905. <https://doi.org/10.1016/j.neuroimage.2008.09.036>.
119. Smith SM, Miller KL, Salimi-Khorshidi G, Webster M, Beckmann CF, Nichols TE, et al. Network modelling methods for fMRI. *Neuroimage*. 2011;54:875–91. <https://doi.org/10.1016/j.neuroimage.2010.08.063>.
120. Ramsey JD, Hanson SJ, Hanson C, Halchenko YO, Poldrack RA, Glymour C. Six problems for causal inference from fMRI. *Neuroimage*. 2010;49:1545–58. <https://doi.org/10.1016/j.neuroimage.2009.08.065>.
121. Patel RS, Bowman FDB, Rilling JK. A Bayesian approach to determining connectivity of the human brain. *Hum Brain Mapp*. 2006;27:267–76. <https://doi.org/10.1002/hbm.20182>.
122. Preti MG, Bolton TA, Van De Ville D. The dynamic functional connectome: state-of-the-art and perspectives. *Neuroimage*. 2017;160:41–54.
123. Calhoun VD, Miller R, Pearson G, Adali T. The chronnectome: time-varying connectivity networks as the next frontier in fMRI data discovery. *Neuron*. 2014;84:262–74.
124. Lindquist MA, Xu Y, Nebel MB, Caffo BS. Evaluating dynamic bivariate correlations in resting-state fMRI: a comparison study and a new approach. *Neuroimage*. 2014;101:531–46.
125. Nolte M, Gal E, Markram H, Reimann MW. Impact of higher order network structure on emergent cortical activity. *Netw Neurosci*. 2019;4:292–314. https://doi.org/10.1162/netn_a_00124.
126. Battiston F, Cencetti G, Iacopini I, Latora V, Lucas M, Patania A, et al. Networks beyond pairwise interactions: structure and dynamics. *Phys Rep*. 2020; <https://doi.org/10.1016/j.physrep.2020.05.004>.
127. Tzourio-Mazoyer N, Landeau B, Papathanassiou D, Crivello F, Etard O, Delcroix N, et al. Automated anatomical labeling of activations in SPM using a macroscopic anatomical parcellation of the MNI MRI single-subject brain. *Neuroimage*. 2002;15:273–89. <https://doi.org/10.1006/nimg.2001.0978>.
128. Desikan RS, Ségonne F, Fischl B, Quinn BT, Dickerson BC, Blacker D, et al. An automated labeling system for subdividing the human cerebral cortex on MRI scans into gyral based regions of interest. *Neuroimage*. 2006;31:968–80.

129. Zalesky A, Fornito A, Harding IH, Cocchi L, Yücel M, Pantelis C, et al. Whole-brain anatomical networks: does the choice of nodes matter? *Neuroimage*. 2010;50:970–83. <https://doi.org/10.1016/j.neuroimage.2009.12.027>.
130. Power JD, Cohen AL, Nelson SM, Wig GS, Barnes KA, Church JA, et al. Functional network organization of the human brain. *Neuron*. 2011;72:665–78. <https://doi.org/10.1016/j.neuron.2011.09.006>.
131. Schaefer A, Kong R, Gordon EM, Laumann TO, Zuo X-N, Holmes AJ, et al. Local-global parcellation of the human cerebral cortex from intrinsic functional connectivity MRI. *Cereb Cortex*. 2018;28:3095–114. <https://doi.org/10.1093/cercor/bhx179>.
132. Fan L, Li H, Zhuo J, Zhang Y, Wang J, Chen L, et al. The human brainnetome atlas: a new brain atlas based on connectional architecture. *Cereb Cortex*. 2016;26:3508–26. <https://doi.org/10.1093/cercor/bhw157>.
133. Bullmore E, Sporns O. Complex brain networks: graph theoretical analysis of structural and functional systems. *Nat Rev Neurosci*. 2009;10:186–98.
134. Rubinov M, Sporns O. Weight-conserving characterization of complex functional brain networks. *Neuroimage*. 2011;56:2068–79. <https://doi.org/10.1016/j.neuroimage.2011.03.069>.
135. Sporns O. Graph theory methods: applications in brain networks. *Dialogues Clin Neurosci*. 2018;20:111–21. <http://www.ncbi.nlm.nih.gov/pubmed/30250388>. Accessed 19 May 2019
136. Suárez LE, Markello RD, Betzel RF, Misis B. Linking structure and function in macroscale brain networks. *Trends Cogn Sci*. 2020;24:302–15. <https://doi.org/10.1016/j.tics.2020.01.008>.
137. Van Den Heuvel MP, Mandl RCW, Kahn RS, Hulshoff Pol HE. Functionally linked resting-state networks reflect the underlying structural connectivity architecture of the human brain. *Hum Brain Mapp*. 2009;30:3127–41. <https://doi.org/10.1002/hbm.20737>.
138. Khalsa S, Mayhew SD, Chechlacz M, Bagary M, Bagshaw AP. The structural and functional connectivity of the posterior cingulate cortex: comparison between deterministic and probabilistic tractography for the investigation of structure-function relationships. *Neuroimage*. 2014;102:118–27. <https://doi.org/10.1016/j.neuroimage.2013.12.022>.
139. Horn A, Ostwald D, Reisert M, Blankenburg F. The structural-functional connectome and the default mode network of the human brain. *Neuroimage*. 2014;102:142–51.
140. Ye Q, Bai F. Contribution of diffusion, perfusion and functional MRI to the disconnection hypothesis in subcortical vascular cognitive impairment. *Neurology*. 2018;3:e000080, 131–9.
141. Bohnen NI, Bogan CW, Müller MLTM. Frontal and periventricular brain white matter lesions and cortical deafferentation of cholinergic and other neuromodulatory axonal projections. *Eur Neurol J* 2009;19:33–50. <http://www.pubmedcentral.nih.gov/articlerender.fcgi?artid=PMC338799>. Accessed 1 July 2020.
142. Egorova N, Dholander T, Khlif MS, Khan W, Werden E, Brodtmann A. Pervasive white matter fiber degeneration in ischemic stroke. *Stroke*. 2020;51:1507–13. <https://doi.org/10.1161/STROKEAHA.119.028143>.
143. Smith RE, Tournier JD, Calamante F, Connelly A. Anatomically-constrained tractography: improved diffusion MRI streamlines tractography through effective use of anatomical information. *Neuroimage*. 2012;62:1924–38. <https://doi.org/10.1016/j.neuroimage.2012.06.005>.
144. Waller R, Dotterer HL, Murray L, Maxwell AM, Hyde LW. White-matter tract abnormalities and antisocial behavior: a systematic review of diffusion tensor imaging studies across development. *NeuroImage: Clinical*. 2017;14:201–15. <https://doi.org/10.1016/j.nicl.2017.01.014>.
145. Bassett DS, Bullmore ET. Small-world brain networks revisited. *Neuroscientist*. 2017;23:499–516.
146. Bressler SL, Menon V. Large-scale brain networks in cognition: emerging methods and principles. *Trends Cogn Sci*. 2010;14:277–90.
147. Postle BR. Working memory as an emergent property of the mind and brain. *Neuroscience*. 2006;139:23–38.
148. Petersen M, Frey BM, Schlemm E, Mayer C, Hanning U, Engelke K, et al. Network localisation of white matter damage in cerebral small vessel disease. *Sci Rep*. 2020;10:1–9. <https://doi.org/10.1038/s41598-020-66013-w>.
149. Cheng B, Schlemm E, Schulz R, Boenstrup M, Messé A, Hilgetag C, et al. Altered topology of large-scale structural brain networks in chronic stroke. *Brain Commun*. 2019;1 <https://doi.org/10.1093/braincomms/fcz020>.
150. Schlemm E, Schulz R, Bönstrup M, Krawinkel L, Fiehler J, Gerloff C, et al. Structural brain networks and functional motor outcome after stroke—a prospective cohort study. *Brain Commun*. 2020;2:fcaa001. <https://doi.org/10.1093/braincomms/fcaa001>.
151. Pantoni L. Cerebral small vessel disease: from pathogenesis and clinical characteristics to therapeutic challenges. *Lancet Neurol*. 2010;9:689–701.
152. Van Dijk EJ, Prins ND, Vrooman HA, Hofman A, Koudstaal PJ, Breteler MMB. Progression of cerebral small vessel disease in relation to risk factors and cognitive consequences: Rotterdam scan study. *Stroke*. 2008;39:2712–9. <https://doi.org/10.1161/STROKEAHA.107.513176>.
153. Østergaard L, Engedal TS, Moreton F, Hansen MB, Wardlaw JM, Dalkara T, et al. Cerebral small vessel disease: capillary pathways to stroke and cognitive decline. *J Cerebral Blood Flow Metab*. 2016;36:302–25. <https://doi.org/10.1177/0271678X15606723>.
154. Wardlaw JM, Smith C, Dichgans M. Small vessel disease: mechanisms and clinical implications. *Lancet Neurol*. 2019;18:684–96. [https://doi.org/10.1016/S1474-4422\(19\)30079-1](https://doi.org/10.1016/S1474-4422(19)30079-1).
155. Takamura T, Hanakawa T. Clinical utility of resting-state functional connectivity magnetic resonance imaging for mood and cognitive disorders. *J Neural Transm*. 2017;124:821–39. <https://doi.org/10.1007/s00702-017-1710-2>.
156. Farràs-Permanyer L, Guàrdia-Olmos J, Peró-Cebollero M. Mild cognitive impairment and fMRI studies of brain functional connectivity: the state of the art. *Front Psychol*. 2015;6:1095. <https://doi.org/10.3389/fpsyg.2015.01095>.
157. Anticevic A, Cole MW, Murray JD, Corlett PR, Wang XJ, Krystal JH. The role of default network deactivation in cognition and disease. *Trends Cogn Sci*. 2012;16:584–92.
158. Hampson M, Driesen NR, Skudlarski P, Gore JC, Constable RT. Brain connectivity related to working memory performance. *J Neurosci*. 2006;26:13338–43. <https://doi.org/10.1523/JNEUROSCI.3408-06.2006>.
159. Silton RL, Heller W, Towers DN, Engels AS, Spielberg JM, Edgar JC, et al. The time course of activity in dorsolateral prefrontal cortex and anterior cingulate cortex during top-down attentional control. *Neuroimage*. 2010;50:1292–302.
160. Menon V. Large-scale brain networks and psychopathology: a unifying triple network model. *Trends Cogn Sci*. 2011;15:483–506.
161. Nekovarova T, Fajnerova I, Horacek J, Spaniel F. Bridging disparate symptoms of schizophrenia: a triple network dysfunction theory. *Front Behav Neurosci*. 2014;171. doi:<https://doi.org/10.3389/fnbeh.2014.00171>.
162. Sridharan D, Levitin DJ, Menon V. A critical role for the right fronto-insular cortex in switching between central-executive and default-mode networks. *Proc Natl Acad Sci U S A*. 2008;105:12569–74. <https://doi.org/10.1073/pnas.0800005105>.
163. Balthazar MLF, Pereira FRS, Lopes TM, da Silva EL, Coan AC, Campos BM, et al. Neuropsychiatric symptoms in Alzheimer's disease are related to functional connectivity alterations in the salience network. *Hum Brain Mapp*. 2014;35:1237–46. <https://doi.org/10.1002/hbm.22248>.
164. He X, Qin W, Liu Y, Zhang X, Duan Y, Song J, et al. Abnormal salience network in normal aging and in amnesic mild cognitive impairment and Alzheimer's disease. *Hum Brain Mapp*. 2014;35:3446–64. <https://doi.org/10.1002/hbm.22414>.
165. Badhwar AP, Tam A, Dansereau C, Orban P, Hoffstaedter F, Bellec P. Resting-state network dysfunction in Alzheimer's disease: a systematic review and meta-analysis. *Alzheimer's Dement Diagnosis Assess Dis Monit*. 2017;8:73–85.
166. Dey AK, Stamenova V, Bacopulos A, Jeyakumar N, Turner GR, Black SE, et al. Cognitive heterogeneity among community-dwelling older adults with cerebral small vessel disease. *Neurobiol Aging*. 2019;77:183–93.
167. Pinter D, Enzinger C, Fazekas F. Cerebral small vessel disease, cognitive reserve and cognitive dysfunction. *J Neurol*. 2015;262:2411–9. <https://doi.org/10.1007/s00415-015-7776-6>.
168. Barulli D, Stern Y. Efficiency, capacity, compensation, maintenance, plasticity: emerging concepts in cognitive reserve. *Trends Cogn Sci*. 2013;17:502–9.
169. Kim HW, Hong J, Jeon JC. Cerebral small vessel disease and Alzheimer's disease: a review. *Front Neurol*. 2020;11:927. <https://doi.org/10.3389/fneur.2020.00927>.
170. Ciric R, Wolf DH, Power JD, Roalf DR, Baum GL, Ruparel K, et al. Benchmarking of participant-level confound regression strategies for the control of motion artifact in studies of functional connectivity. *Neuroimage*. 2017;154:174–87.
171. Ciric R, Rosen AFG, Erus G, Cieslak M, Adebimpe A, Cook PA, et al. Mitigating head motion artifact in functional connectivity MRI. *Nat Protoc*. 2018;13:2801–26. <https://doi.org/10.1038/s41596-018-0065-y>.
172. Li J, Kong R, Liégeois R, Orban C, Tan Y, Sun N, et al. Global signal regression strengthens association between resting-state functional

- connectivity and behavior. *Neuroimage*. 2019;196:126–41. <https://doi.org/10.1016/j.neuroimage.2019.04.016>.
173. Telesford QK, Morgan AR, Hayasaka S, Simpson SL, Barret W, Kraft RA, et al. Reproducibility of graph metrics in fMRI networks. *Front Neuroinform*. 2010; 117. doi:<https://doi.org/10.3389/fninf.2010.00117>.
 174. Braun U, Plichta MM, Esslinger C, Sauer C, Haddad L, Grimm O, et al. Test-retest reliability of resting-state connectivity network characteristics using fMRI and graph theoretical measures. *Neuroimage*. 2012;59:1404–12.
 175. Wang JH, Zuo XN, Gohel S, Milham MP, Biswal BB, He Y. Graph theoretical analysis of functional brain networks: test-retest evaluation on short- and long-term resting-state functional MRI data. *PLoS One*. 2011;6:e21976. <https://doi.org/10.1371/journal.pone.0021976>.
 176. Zuo XN, Kelly C, Adelstein JS, Klein DF, Castellanos FX, Milham MP. Reliable intrinsic connectivity networks: test-retest evaluation using ICA and dual regression approach. *Neuroimage*. 2010;49:2163–77.
 177. Choe AS, Jones CK, Joel SE, Muschelli J, Belegu V, Caffo BS, et al. Reproducibility and temporal structure in weekly resting-state fMRI over a period of 3.5 years. *PLoS One*. 2015;10:e0140134. <https://doi.org/10.1371/journal.pone.0140134>.
 178. Pinter D, Beckmann C, Koini M, Pirker E, Filippini N, Pichler A, et al. Reproducibility of resting state connectivity in patients with stable multiple sclerosis. *PLoS One*. 2016;11:e0152158. <https://doi.org/10.1371/journal.pone.0152158>.
 179. Abrol A, Damaraju E, Miller RL, Stephen JM, Claus ED, Mayer AR, et al. Replicability of time-varying connectivity patterns in large resting state fMRI samples. *Neuroimage*. 2017;163:160–76.
 180. Song J, Desphande AS, Meier TB, Tudorascu DL, Vergun S, Nair VA, et al. Age-related differences in test-retest reliability in resting-state brain functional connectivity. *PLoS One*. 2012;7 <https://doi.org/10.1371/journal.pone.0049847>.
 181. Guo CC, Kurth F, Zhou J, Mayer EA, Eickhoff SB, Kramer JH, et al. One-year test-retest reliability of intrinsic connectivity network fMRI in older adults. *Neuroimage*. 2012;61:1471–83. <https://doi.org/10.1016/j.neuroimage.2012.03.027>.
 182. Shabir O, Berwick J, Francis SE. Neurovascular dysfunction in vascular dementia, Alzheimer's and atherosclerosis. *BMC Neurosci*. 2018;19:62. <https://doi.org/10.1186/s12868-018-0465-5>.
 183. Fabiani M, Gordon BA, Maclin EL, Pearson MA, Brumback-Peltz CR, Low KA, et al. Neurovascular coupling in normal aging: a combined optical, ERP and fMRI study. *Neuroimage*. 2014;85 0 1:592–607. doi:<https://doi.org/10.1016/j.neuroimage.2013.04.113>.
 184. Tsvetanov KA, Henson RNA, Rowe JB. Separating vascular and neuronal effects of age on fMRI BOLD signals. *Philos Trans R Soc B Biol Sci*. 2019;376: 20190631. <https://doi.org/10.1098/rstb.2019.0631>.
 185. Hatazawa J, Shimosegawa E, Satoh T, Toyoshima H, Okudera T. Subcortical hypoperfusion associated with asymptomatic white matter lesions on magnetic resonance imaging. *Stroke*. 1997;28(10):1944–7.
 186. Joutel A, Monet-Leprêtre M, Gosele C, Baron-Menguy C, Hammes A, Schmidt S, et al. Cerebrovascular dysfunction and microcirculation rarefaction precede white matter lesions in a mouse genetic model of cerebral ischemic small vessel disease. *J Clin Invest*. 2010;120(2):433–45.
 187. Kuwabara Y, Ichiya Y, Sasaki M, Yoshida T, Fukumura T, Masuda K, et al. Cerebral blood flow and vascular response to hypercapnia in hypertensive patients with leukoaraiosis. *Ann Nucl Med*. 1996;10:293–8.
 188. Purkayastha S, Fadar O, Mehregan A, Salat DH, Moscufo N, Meier DS, et al. Impaired cerebrovascular hemodynamics are associated with cerebral white matter damage. *J Cereb Blood Flow Metab*. 2014;34(2):228–34.
 189. Thomas BP, Liu P, Park DC, Van Osch MJP, Lu H. Cerebrovascular reactivity in the brain white matter: magnitude, temporal characteristics, and age effects. *J Cereb Blood Flow Metab*. 2014;34(2):242–7.
 190. Golestani AM, Kwintu JB, Strother SC, Khatamian YB, Chen JJ. The association between cerebrovascular reactivity and resting-state fMRI functional connectivity in healthy adults: the influence of basal carbon dioxide. *Neuroimage*. 2016;132:301–13.
 191. Song F, Khan KS, Dinnes J, Sutton AJ. Asymmetric funnel plots and publication bias in meta-analyses of diagnostic accuracy. *Int J Epidemiol*. 2002;31:88–95. <https://doi.org/10.1093/ije/31.1.88>.
 192. Karim HT, Andreescu C, Tudorascu D, Smagula SF, Butters MA, Karp JF, et al. Intrinsic functional connectivity in late-life depression: trajectories over the course of pharmacotherapy in remitters and non-remitters. *Mol Psychiatry*. 2017;22:450–7. <https://doi.org/10.1038/mp.2016.55>.
 193. Taylor WD, Aizenstein HJ, Alexopoulos GS. The vascular depression hypothesis: mechanisms linking vascular disease with depression. *Mol Psychiatry*. 2013;18:963–74. <https://doi.org/10.1038/mp.2013.20>.
 194. Kenny ER, O'Brien JT, Cousins DA, Richardson J, Thomas AJ, Firbank MJ, et al. Functional connectivity in late-life depression using resting-state functional magnetic resonance imaging. *Am J Geriatr Psychiatry*. 2010;18:643–51.
 195. Bohr IJ, Kenny E, Blamire A, O'Brien JT, Thomas AJ, Richardson J, et al. Resting-state functional connectivity in late-life depression: higher global connectivity and more long distance connections. *Front Psychiatry*. 2013; 116 <https://doi.org/10.3389/fpsy.2012.00116>.
 196. Alexopoulos GS, Hoptman MJ, Yuen G, Kanellopoulos D, K. Seirup J, Lim KO, et al. Functional connectivity in apathy of late-life depression: a preliminary study. *J Affect Disord* 2013;149:398–405. doi:<https://doi.org/10.1016/j.jad.2012.11.023>.
 197. Joo SH, Lee CU, Lim HK. Apathy and intrinsic functional connectivity networks in amnesic mild cognitive impairment. *Neuropsychiatr Dis Treat*. 2017;13:61–7. <https://doi.org/10.2147/NDT.S123338>.
 198. Moretti R, Signori R. Neural correlates for apathy: frontal-prefrontal and parietal cortical-subcortical circuits. *Front Aging Neurosci*. 2016;289 <https://doi.org/10.3389/fnagi.2016.00289>.
 199. Karim HT, Rosso A, Aizenstein HJ, Bohnen NI, Studenski S, Rosano C. Resting state connectivity within the basal ganglia and gait speed in older adults with cerebral small vessel disease and locomotor risk factors. *NeuroImage Clin*. 2020;28 <https://doi.org/10.1016/j.nicl.2020.102401>.
 200. Meeker KL, Wisch JK, Hudson D, Coble D, Xiong C, Babulal GM, et al. Socioeconomic status mediates racial differences seen using the AT(N) framework. *Ann Neurol*. 2021;89:254–65. <https://doi.org/10.1002/ana.25948>.

Publisher's Note

Springer Nature remains neutral with regard to jurisdictional claims in published maps and institutional affiliations.

Ready to submit your research? Choose BMC and benefit from:

- fast, convenient online submission
- thorough peer review by experienced researchers in your field
- rapid publication on acceptance
- support for research data, including large and complex data types
- gold Open Access which fosters wider collaboration and increased citations
- maximum visibility for your research: over 100M website views per year

At BMC, research is always in progress.

Learn more biomedcentral.com/submissions

